

## GAS AND STARS IN AN HI-SELECTED GALAXY SAMPLE

JESSICA L. ROSENBERG<sup>1, 2</sup>

Center for Astrophysics & Space Astronomy, Department of Astrophysical and Planetary Sciences, University of Colorado, Boulder, CO 80309

STEPHEN E. SCHNEIDER

Department of Astronomy, University of Massachusetts, Amherst, MA 01003

JENNIFER POSSON-BROWN<sup>2</sup>

Smith College, Northampton, MA 01063

*Draft version April 15, 2019*

### ABSTRACT

We present the results of a J-band study of the HI-selected Arecibo Dual-Beam Survey and Arecibo Slice Survey galaxy samples using the 2 Micron All-Sky Survey data. We find that these galaxies span a wide range of stellar and gas properties. However, despite the diversity within the samples, we find a very tight correlation between luminosity and size in the J-band, similar to that we previously found (Rosenberg & Schneider 2003) between the HI mass and size. We also find that the correlation between the baryonic mass and the J-band diameter is even tighter than between the baryonic mass and the rotational velocity.

*Subject headings:* galaxies:fundamental parameters — galaxies: stellar content — infrared: galaxies

### 1. INTRODUCTION

In recent years several large “blind” 21 cm surveys for galaxies have been conducted providing a measurement of the gas in galaxies in the local universe (Meyer et al. 2004; Rosenberg & Schneider 2000; Zwaan et al. 1997, Spitzak & Schneider 1998). These surveys have revealed many galaxies with unusual characteristics: some without a definite optical counterpart and others with very high HI to stellar mass ratios, for example. These galaxy samples give us an opportunity to explore how the stellar properties of gas-rich galaxies differ from those of optically luminous systems.

Our understanding of the relationship between the global properties of gas and stars in galaxies has mostly been driven by studies of optically-selected, high surface brightness galaxies (e.g. Scodreggio & Gavazzi 1993; Huchtmeier & Richter 1985; Fisher & Tully 1981). Various efforts have been made to extend these studies to lower surface brightness galaxies, (e.g., Galaz et al. 2002, McGaugh et al. 2000, O’Neil et al. 2000, Sprayberry et al. 1995) revealing a great diversity of properties outside of the traditional “norms” defined by the high surface brightness samples, but such surveys remain tied to the requirement that the galaxies have formed stars in sufficient numbers and surface densities to be detected optically. Extragalactic HI surveys provide one of the few ways to probe the galaxy population independent of their luminosity and surface brightness. HI galaxy selection is also complementary to optical galaxy selection with respect to star formation history since the conversion of gas to stars renders a galaxy more visible optically, but less visible in an HI survey.

The blind HI surveys conducted with the Arecibo radio telescope remain among the deepest to date sampling galaxies with HI fluxes almost an order of magnitude smaller than the very large, but shallow HI Parkes All-Sky Survey (HIPASS, Meyer et al. 2004) and probing the lowest mass galaxies over a wider range of environments. The stellar properties of the Arecibo samples of Zwaan et al (1997) and Spitzak & Schneider (1998) have been studied at optical wavelengths. These studies have provided a picture of the gas-rich galaxies in the universe as containing a sub-sample of low-luminosity and low-surface-brightness galaxies (Spitzak & Schneider 1998) in higher proportion than found in optical surveys.

Infrared observations more nearly reflect the total stellar mass of galaxies, since they are less sensitive to the star formation rate and history and are less affected by dust than optical observations. In this paper we use the data from the 2 Micron All-Sky Survey (2MASS) to study the infrared properties of galaxies from the Arecibo Dual-Beam Survey (Rosenberg & Schneider 2000; RS) and from the Slice Survey (Spitzak & Schneider 1998; SS). Both of these surveys are “blind” HI surveys that probed the gas-rich galaxy populations in the local universe. The 2MASS observations of this galaxy sample are useful for examining the relationship between gas and stars in gas-rich galaxies in the local universe. While 2MASS provides information about the stellar mass in these galaxies, it suffers from a lack of surface brightness sensitivity which limits the galaxy detection rate. Nevertheless, over 85% of the galaxies in each sample were detected.

We discuss the HI and 2MASS data used in this study in §2 along with details about how some of the galaxies were measured from the 2MASS images. In §3 we discuss the relationship between the gaseous and stellar properties of the galaxies and discuss the surface densities of

<sup>1</sup> National Science Foundation Astronomy and Astrophysics Postdoctoral Fellow

<sup>2</sup> Present address: Center for Astrophysics, Cambridge, MA 02138

gas and stars in §4. In §5 we discuss the 2MASS images of the galaxies and in §6 we summarize our results.

## 2. DATA

### 2.1. Sample Selection - The Arecibo Dual-Beam and Slice Surveys

We examine the stellar properties of two HI-selected galaxy samples. Both the RS and SS surveys are “blind” 21 cm surveys carried out with the Arecibo 305 m telescope prior to the Gregorian upgrade. We have used these surveys to identify galaxies purely based on their gas content out to  $7977 \text{ km s}^{-1}$  and  $8340 \text{ km s}^{-1}$  respectively. The RS survey covered  $\sim 430 \text{ deg}^2$  in the main beam and detected 265 galaxies while the SS survey covered  $\sim 55 \text{ deg}^2$  and detected 75 galaxies. The selection functions and HI mass functions have been studied in detail and are presented in Rosenberg & Schneider (2002) and Schneider, Spitzak, & Rosenberg (1999) for the RS and SS surveys respectively.

The details of the calculations of line width, velocity, distance, and HI mass for the entire sample are presented in RS. The SS survey additionally includes broadband B, R and I optical data. There are three galaxies from the RS survey for which the RS line widths differed from the literature values because one horn of the velocity profile was missed in the survey measurement. In these cases (RS 17, RS 109, and RS 189) we use the values from the Huchtmeier & Richter catalog (1985) when using line widths to calculate the dynamical mass (see §3).

### 2.2. The 2-Micron All Sky Survey Data

The 2 Micron All-Sky Survey (2MASS) provides simultaneous J, H, and  $K_s$ -band observations of the entire sky; the 2MASS project processed the data to generate a point source catalog and an extended source catalog. We use the extended source catalog data for the RS and SS galaxies in the following analyses and also supplement this with our own analysis of the images for a number of galaxies that were undetected by the standard processing procedures (discussed in §2.2.1). A full description of the galaxy detection algorithm and the resulting catalogs are available in the Explanatory Supplement to the 2MASS All Sky Data Release<sup>3</sup> (Cutri et al.).

The 2MASS extended source catalog has undergone several iterations and we use results from both the Version 2 and Version 3 catalogs in these analyses. We use Version 2 in addition to Version 3 because this earlier version of the software used previous galaxy catalog positions to seed the search algorithms (in addition to doing an independent automated search) and therefore measured a number of fainter sources that Version 3 did not detect, since it used only the automated algorithms. In addition, there are some large galaxies for which we report the Version 2 values rather than the Version 3 values because some of the information is missing in the version 3 catalog.

<sup>3</sup> <http://www.ipac.caltech.edu/2mass/releases/allsky/doc/explsups.html>  
by Cutri, R.M., Skrutskie, M.F., Van Dyk, S., Beichman, C.A., Carpenter, J.M., Chester, T., Cambresy, L., Evans, T., Fowler, J., Gizis, J., Howard, E., Huchra, J., Jarrett, T., Kopan, E.L., Kirkpatrick, J.D., Light, R.M., Marsh, K.A., McCallon, H., Schneider, S., Stiening, R., Sykes, M., Weinberg, M., Wheaton, W.A., Wheelock, S., Zacharias, N.

The J-band observations are the most sensitive of the three 2MASS bands and our HI-selected sources tend to be blue on average, so we use these data in our analyses. The catalog data were used for 45 (4 from Version 2, 41 from Version 3) of the 75 SS galaxies and 180 (50 from Version 2, 130 from Version 3) of the 265 RS galaxies. Some of the galaxies that were not in the extended source catalogs can be identified on the full resolution 2MASS images; in these cases we measured the galaxy from the image. Details of our image analysis are described below. There were an additional 19 SS and 47 RS galaxies that we measured from the images. For 11 of the SS galaxies and 38 of the RS galaxies there was no cataloged detection and we were not able to measure the galaxy from the images. For most of the galaxies that were not measured, the source was just too faint to be detected in the short 2MASS exposures, but some exceptions are described in the specific galaxy notes below.

The near infrared measurements for the galaxies in both the RS and SS surveys are given in Tables 1 and 2 in the Appendix. The tables also list the source for the measurements, i.e., whether the data come from Version 2 or 3 of the 2MASS catalog, were measured from the image, or if the source was not detected.

#### 2.2.1. 2MASS Measured Data

To measure the galaxies on the 2MASS images we have used the ELLIPSE package in IRAF. The brighter galaxies were interactively fit with ellipses such that the ellipse parameters were allowed to change in the highest surface brightness regions but when the fits became uncertain in the outer regions, the ellipse parameters were held fixed while additional steps in radius were taken. For the lowest surface brightness galaxies, even the central regions had uncertain parameter fits, so only fixed circular apertures were used for the photometry.

ELLIPSE was run at least twice for each galaxy so that the outer “background” ellipses could be used for background subtraction. Then the fitting was rerun on the background-subtracted image. The background subtraction was repeated if an adequately flat background had not been obtained on the first pass. In all cases, the point sources in the image were masked prior to the ellipse fitting.

#### 2.2.2. Notes About Selected Galaxies

We provide information about the near infrared measurements for a few galaxies that warrant a comment. The numbers refer to the entry number in the RS survey catalog (see Table 1 for the ADBS names).

- **RS 50:** The HI detection of this system includes an interacting pair of galaxies. Since we do not separate the pair in the HI observation we do not try to correlate the HI with a near infrared measurement of one galaxy or the other.
- **RS 73:** We do not report an infrared measurement for this galaxy because it is too contaminated by a bright star.
- **RS 79:** We use the Version 2 measurement of the brighter galaxy in the interacting pair. Both galaxies are probably contributing to the HI, but includ-

ing the fainter of the two galaxies would change the J-band magnitude by less than 0.3 mag.

- **RS 184:** This galaxy is in the Version 3 extended source catalog. However, we use measurements from the image because the center of this very low surface brightness galaxy was missed in favor of a field star by the galaxy detection algorithm.

### 2.3. Using the 2MASS data as a Measure of Stellar Mass

As a basis for understanding the properties of these HI-selected galaxies we want to compare the gas mass and the stellar mass in these systems. The 2MASS data are particularly good for measuring the stellar mass as they are more sensitive to low mass stars and less sensitive to dust and star formation than optical observations. However, there is substantial scatter in the relationship between luminosity and stellar mass even in the infrared. The scatter can be decreased by using information about the galaxy's color (Bell & de Jong 2001).

Based on stellar population synthesis models, a variety of estimates have been made for various stellar initial mass functions and star-formation histories. Bell & de Jong (2001) present a range of models that yield realistic colors and surface brightnesses for present-day galaxies. Bell (private communication) has provided us with J-band values for these same models and finds a tight correlation between (B-R) color and the ratio of stellar mass to J-band luminosity:

$$\log(M_{\text{star}}/L_J) = 0.552(B - R) - 0.724 \quad (1)$$

The value of  $M_{\text{star}}/L_J$  varies from  $\sim 0.4$  for blue galaxies  $[(B - R) \sim 0.6]$  to  $\sim 1.2$  for red galaxies  $[(B - R) \sim 1.6]$ . Including differences between models and measurement uncertainties, there is thus a range of almost a factor of 4 in the relationship between stellar mass and J-band luminosity for the normal range of galaxy colors. When the color is known, the total range reduces to about a factor of 1.5. These results appear to be consistent with alternative models carried out for I and H bands (cf. McGaugh & de Blok 1997; McGaugh et al. 2000).

The SS galaxies were previously observed in broadband colors, which allows us to estimate their mass-to-light ratios more precisely. Their average (B-R) color was 1.0, so their average  $M_{\text{star}}/L_J$  value is 0.7. Figure 1 shows the relationship between  $M_{\text{star}}/L_J$  for the SS galaxies calculated using Equation 1 and their ratio of HI mass to J-band luminosity,  $M_{\text{HI}}/L_J$ . The total neutral hydrogen mass was calculated from the published data using the well-known relationship  $M_{\text{HI}} = 2.36 \times 10^5 D^2 I_{\text{HI}}$ , where  $D$  is the distance in Mpc and  $I_{\text{HI}}$  is the integrated flux in  $\text{Jy km s}^{-1}$ . The standard deviation around the line is 0.15 while the standard deviation around the average value of  $\log(M_{\text{star}}/L_J) = -0.15$  is 0.19. The correlation is not extremely tight, but it allows us to improve our estimate of the mass-to-light-ratios for the galaxies that do not have broadband colors: the RS galaxies and the faintest SS galaxies.

In addition to the intrinsic and measurement uncertainties in determining  $M_{\text{star}}/L_J$ , an additional source of scatter is introduced in the determination of stellar

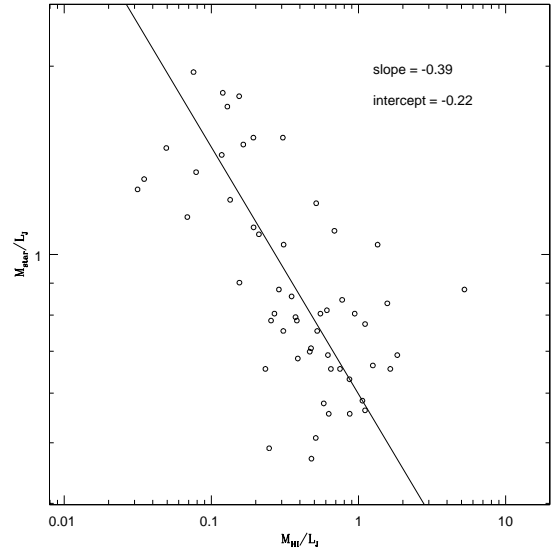


FIG. 1.— The relationship between the mass-to-light ratio calculated using Equation 1 and the  $M_{\text{HI}}/L_J$  for the SS data. The fit to these data are used to improve the estimate of  $M_{\text{star}}/L_J$  for the data for which B-R measurements are not available.

mass because the 2MASS data are not very deep. Uncertainties in the J-band flux are caused by the difficulty in measuring the isophotal sizes near the limit of the survey surface brightness sensitivity, particularly for the lowest surface brightness galaxies. We compare the isophotal measurements of galaxy magnitudes at  $21 \text{ mag arcsec}^{-2}$  to the measurements in the largest aperture before the noise takes over (i.e., before the values start oscillating between fainter and brighter values due to noise). For the 2MASS cataloged values, we use the brightest aperture value reported. To be consistent with the catalog measurements, we restrict our own measured apertures to those used in the catalog (i.e., 5, 7, 10, 15, 20, 25, 30, 40, 50, 60, or 70 arcsec). However, 19 of the RS galaxies are significantly larger than  $70''$  so the largest aperture is not a good measurement of its size of flux. For these galaxies, we use the extrapolated J-band magnitude so that the size and flux are not severely underestimated. Table 1 indicates for which galaxies the extrapolated values are used. There are no SS galaxies that are significantly larger than the  $70''$  aperture.

Figure 2 shows that the magnitudes for most of the faint galaxies are severely underestimated if the isophotal value is used. For all of the J-band luminosities in this paper we use the aperture measurement values. Additionally, we adopt a value of  $M_{\odot}(\text{J}) = 3.73$  (Johnson 1966; Allen 1973) for our conversion to solar luminosities.

### 3. STARS AND GAS IN AN HI-SELECTED SAMPLE

By using the RS and SS data, we have selected a wide range of galaxy types with the only criteria being that they contain neutral hydrogen. These systems span the range from dwarfs and irregulars to early-type spirals and interacting systems. Appendix A shows the 2MASS near infrared images for these galaxies; their morphology is discussed in greater detail in §5.

Figure 3 shows the relationship between the J-band surface brightness and  $M_{\text{HI}}/L_J$  for the RS galaxies (filled circles) and for the SS galaxies (open circles). The J-

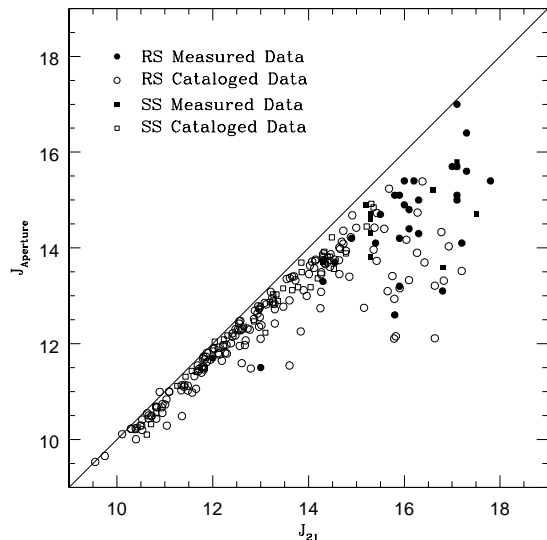


FIG. 2.— The relationship between aperture and 21 mag arcsec<sup>-2</sup> isophotal magnitudes from the RS and the SS samples. The open symbols indicate magnitudes that were obtained from the 2MASS extended source catalog, Version 2 or 3. The closed symbols indicate magnitudes that were measured from the images.

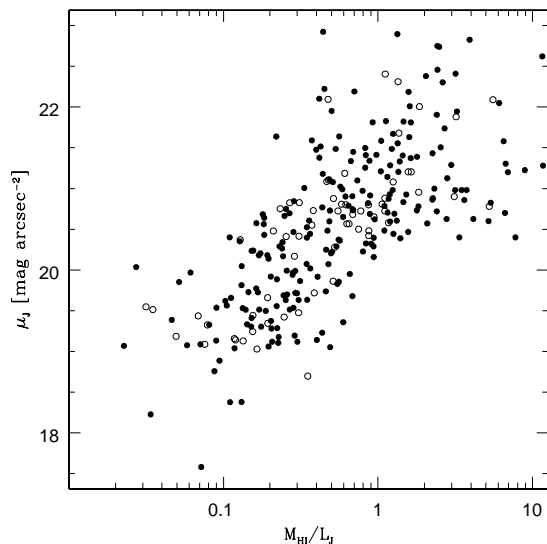


FIG. 3.— The relationship between the average J-band surface brightness and the ratio of HI mass to J-band luminosity for the RS galaxies (filled circles) and the SS galaxies (open circles).

band surface brightness is determined within the aperture radius (or extrapolated radius for the largest galaxies) determined as discussed in the previous section. The surface brightness that we derive is, roughly, a surface brightness at a slightly fainter isophote than  $J=21$  mag arcsec<sup>-2</sup>. This figure illustrates that, in general, the gas-rich galaxies (galaxies with high values of  $M_{HI}/L_J$ ) are the lower surface brightness ones indicating that HI-selection is a good way to find low surface brightness galaxies. Despite not having a very precise measure of surface brightness, the correlation with  $M_{HI}/L_J$  is pretty good.

The typical (B-J) color for a spiral galaxy is between 2 and 3. Using (B-J) = 2 as a conservative value, the

average surface brightnesses of these HI selected galaxies range between  $\Sigma_J = 18$  to 25 mag arcsec<sup>-2</sup>. There are a variety of different definitions of what constitutes a low surface brightness galaxy. One definition refers only to the central surface brightness of the disk component after a bulge-disk decomposition has been carried out. By this definition, many galaxies with high surface brightness bulges are categorized as LSB, because the disk component is faint. Another common definition uses the mean blue surface brightness within the  $\mu_{B_0} = 25.0$  mag arcsec<sup>-2</sup> isophote, giving the label of LSB to galaxies with inclination-corrected mean surface brightnesses dimmer than  $\langle \mu_{B_0} \rangle > 25.0$  mag arcsec<sup>-2</sup>.

Since we cannot perform bulge-disk decompositions with the present data, our mean J-band surface brightnesses within the  $\mu_J = 21.0$  mag arcsec<sup>-2</sup> are most readily comparable to the latter definition, although for typical (B-J) colors we measure the mean within a brighter isophote. It appears, though, that analogous to the B-band definition of LSB, we might call galaxies dimmer than  $\langle \mu_J \rangle > 21.0$  mag arcsec<sup>-2</sup> infrared LSBs. This cut-off for LSBs also marks the approximate point at which the total stellar luminosity becomes smaller than the HI mass (in solar units).

The total baryonic mass was estimated from the HI and J-band emission using:

$$M_{bar} = M_{star} + 1.4 \times M_{HI}. \quad (2)$$

where  $M_{star}$  is the total stellar mass, derived from the J-band luminosity mass-to-light ratio discussed in the previous section, and the total gas mass is estimated from  $M_{HI}$  multiplied by 1.4 to account for helium and metals. Obviously, including an estimate of the molecular and ionized gas would increase this further. The stellar and gas masses both have significant uncertainties associated with them (e.g., due to the metallicity of the stars and the amount of molecular gas present), but the effect of internal extinction on the estimate is small compared to its effect at optical wavelengths since the extinction at J is only about 20% of that at B. Furthermore, the additional gas mass is likely to be largest for earlier type galaxies (Young & Knezek 1991), which are dominated by their stellar content, and the uncertainties in the stellar mass are largest for the dim galaxies that are generally dominated by their neutral hydrogen mass, so the uncertainties should have little impact on the total baryonic mass estimates.

Figure 4 shows how the various measured and derived values of mass and luminosity vary with  $M_{HI}/L_J$ . We find that the HI mass is essentially uncorrelated with the ratio for our HI-selected sample; consequently, the stellar luminosity declines roughly in inverse proportion to the  $M_{HI}/L_J$  ratio. An indication of dynamical mass was calculated for our galaxies using their HI line widths (see RS and SS for a discussion of the measurements of line width) and optical dimensions to estimate the inclination and rotation speed, using the equation:

$$M_{dyn} = v_{rot}^2 r_{opt} / G. \quad (3)$$

$v_{rot}$  is the inclination corrected line width ( $v/\sin[i]$ ). We limited the inclination correction to inclinations greater than  $i > 66^\circ$  ( $b/a \leq 0.4$ ). This calculation of dynamical mass will not accurately estimate the masses

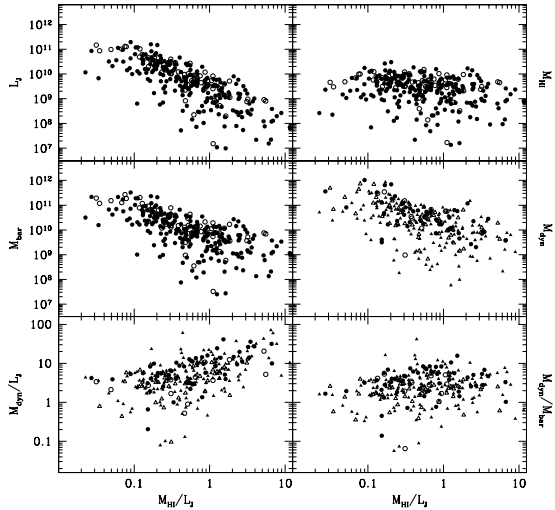


FIG. 4.— The dependence of stellar luminosity, HI mass, total baryonic mass, and dynamical mass upon the ratio of gas to stars. The distance independent quantities of the ratio of dynamical mass to J-band luminosity and the ratio of dynamical mass to baryonic mass are also plotted as a function of the gas to stars ratio. The filled circles are the RS galaxies, the open circles are the SS galaxies. The triangles plotted in panels containing dynamical mass are the galaxies for which  $b/a > 0.4$  for which the dynamical mass measurements may not be reliable.

of dwarf systems that are not primarily rotationally supported, and this mass estimate is directly dependent on the limits to which starlight is seen, but will, nevertheless give an indication of the total mass inside the faintest detected isophote. We have chosen to use the optical size in this calculation, despite the fact that there is often significant HI mass outside of this radius, because HI sizes are only available for a small subset of the RS data and are not available for any of the SS data. The optical sizes of the RS galaxies are derived from Palomar Sky Survey images and represent roughly the B-band 25 mag arcsec<sup>-2</sup> isophotal size. In Figure 4 the galaxies with  $b/a > 0.4$  (more face-on systems for which the determination of dynamical mass is much less reliable) have been plotted as triangles.

Even though there are some clear trends in the properties of the galaxies in these surveys, Figure 4 also illustrates an important diversity. The width of the distribution of masses, luminosities and mass-to-light ratios at any given value of  $M_{HI}/L_J$  is many times larger than might be caused by measurement uncertainties alone. The spread is probably even larger than these figures show since the lower-mass sources were only detectable to a limited distance within our search volume. What Figure 4 shows is that galaxies of any given HI mass span the entire range of gas-to-star ratios – we see galaxies that are low in  $M_{HI}$  because they have turned most of their gas into stars and some that have low  $M_{HI}$  because they are low mass systems with little of their mass in stars.

We note the scarcity of galaxies with  $M_{HI}/L_J \lesssim 0.03$  in Figure 4. It is not clear whether this scarcity is a selection effect or a true deficit of galaxies. Presumably, some ellipticals and lenticulars would fall in this range, and some early-type systems *were* detected in these surveys. The total contribution of early type galaxies containing HI is

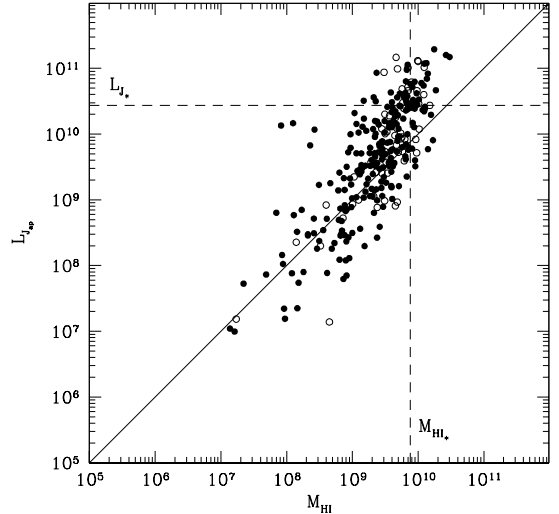


FIG. 5.— The relationship between the J-band luminosity and HI mass for the RS (filled circles) galaxies and the SS (open circles) galaxies. The dashed lines indicate  $M_{HI*}$  (Rosenberg & Schneider 2002) and  $L_{J*}$  (from the 2dF sample using 2MASS measurements; Cole et al. 2001). The solid line indicates a one-to-one relationship between the parameters.

uncertain. At such low  $M_{HI}/L_J$  values, the HI selection criteria only permit us to detect high stellar luminosity sources, and even those only out to a relatively small distances. HI data for an unbiased optical sample is needed to determine their true statistical contribution.

The large range of galaxy properties and  $M_{HI}/L_J$  values for the RS and SS surveys indicates that there is not an easy conversion between the HI mass function and the J-band luminosity function. Figure 5 further demonstrates the problem with using one of these parameters to predict the other. It is not clear that there is a linear relationship between  $L_J$  and  $M_{HI}$  at all masses and luminosities and the spread around the correlation between the quantities is large. As we noted in our earlier paper (Rosenberg & Schneider 2002), at a given HI mass, there may be several orders of magnitude variation in the J-band luminosity, making HI mass a poor predictor of stellar content, and vice versa.

Both the baryonic and dynamical mass estimates are higher for sources with smaller ratios of  $M_{HI}/L_J$ . As we show in Figure 4, however, the dynamical mass-to-light ratio is higher on average for the gas-rich galaxies. This figure also shows that the ratio of dynamical mass to baryonic mass is relatively flat as function of  $M_{HI}/L_J$  with a median value of 3.8 for galaxies with  $b/a < 0.4$ . The range in values that that we find for  $M_{dyn}/M_{bar}$  is comparable to the range for disk galaxies (Zavala et al. 2003). Even excluding the more face-on systems for which the dynamical mass calculation is problematic, there are 5 galaxies with dynamical masses that are smaller than their baryonic mass estimate. For 2 of the RS cases, the measurement of inclination is for the bright central region, but there is a more diffuse light distribution that may indicate that these systems are more face on. For the other 3 systems it is not clear why the dynamic mass is much smaller than the baryonic mass except that they seem to have low rotation velocities for such edge-on systems that might indicate that the line

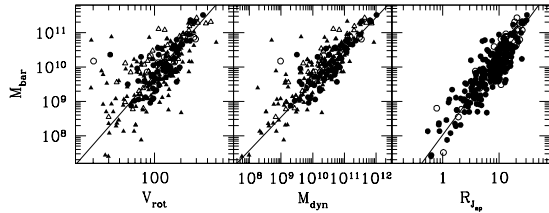


FIG. 6.— The baryonic mass for the ADBS galaxies (filled circles) and the AS galaxies (open circles) plotted against the dynamic mass, rotational velocity, and J-band size. The triangles in the dynamic mass and rotational velocity plots indicate the galaxies for which  $b/a \geq 0.4$  and are, therefore, less reliable. The solid lines in the plots show the average of forward and backward least squares fits to the data excluding the galaxies with  $b/a \geq 0.4$ .

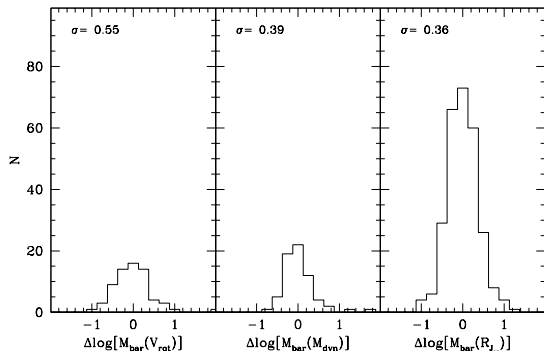


FIG. 7.— The scatter of the baryonic masses around the least squares fits to each of the quantities shown in Figure 6. The rms dispersion of the fit is noted at the top of each panel.

width has not been properly measured (e.g., missing one horn of a double horned HI profile).

Figure 6 shows the relationship between our estimate of the baryonic mass and a variety of other measurements that relate to the overall mass of a galaxy: the dynamical mass (as described in §3), the rotation speed, and the radius. Note that we have marked the face-on ( $b/a \geq 0.4$ ) galaxies with triangles and have not included them in the fits.

It is apparent by eye that the scatter is significantly smaller for galaxy radius than for other more traditional estimators of mass, although when we remove the more face-on galaxies from our calculation, the difference between the dynamical mass and J-band size is greatly reduced. We averaged forward and backward linear least squares fits to these data and display the distribution around the fit and the calculated sigma in Figure 7. Thus, the size of a galaxy makes a good predictor of the mass present. While galaxy models do indicate that size might be the third parameter in a spiral galaxy fundamental plane relationship (Shen, Mo, & Shu 2002), the physics behind this correlation is unclear.

#### 4. THE SURFACE DENSITY OF MATTER IN GALAXIES

Despite the diverse range in galaxy properties discussed in the previous sections, there is a tight correlation between HI mass and HI size (Rosenberg & Schneider 2003) as well as a good correlation between J-band luminosity and J-band size. We examine the mass surface densities of gas, stars, and baryons since the Schmidt Law associates the surface density of gas in a galaxy with

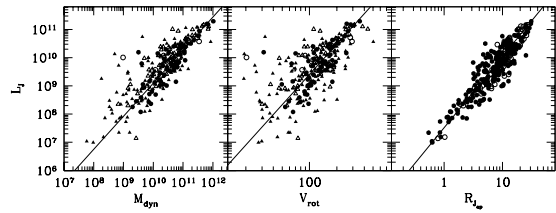


FIG. 8.— The J-band luminosity for the RS galaxies (filled circles) and the SS galaxies (open circles) plotted against the dynamical mass, rotational velocity, and J-band size. The triangles in the dynamical mass and rotational velocity plots indicate the galaxies with  $b/a \geq 0.4$ . The solid lines show the forward and backward least squares fits to the data excluding galaxies with  $b/a \geq 0.4$ .

the star formation rate (Kennicutt 1998) and seems to imply a regulation mechanism between the gas and the star formation that might help explain the relationship between mass and size for these two populations.

Figure 8 shows the relationship between luminosity and dynamical mass, rotational velocity, and J-band size for these galaxies. Forward and backward linear least squares fits to these data are plotted. The standard deviation around these fits are 0.49, 0.69, and 0.37 respectively, providing an indication of the significance of the  $R_J$  versus  $L_J$  correlation. For the dynamical mass and rotational velocity correlations we have plotted the galaxies with axis ratios greater than 0.4 as circles (galaxies with axis ratios of 0.4 or less are plotted as triangles). We have only included those galaxies with axis ratios greater than 0.4 in these two fits.

The relationship between J-band luminosity and J-band size is tighter than the Tully-Fisher relationship (Tully & Fisher 1977) for this sample which includes irregulars, interacting systems, and dwarfs as well as spirals. Unfortunately, since luminosity and size scale the same way with distance, the tight correlation does not offer any possibilities for distance estimation.

The Tully-Fisher relation (Tully & Fisher 1977) has provided an important test of galaxy formation simulations and has been very hard to reproduce in detail; most of the galaxies produced in simulations lose too much of their angular momentum without large amounts of ad hoc energy injection into the system. Governato et al. (2004) have managed to produce one galaxy with the correct dynamical properties by going to higher resolution in their simulations, but still has an excess of massive satellites and a paucity of cold gas. Even as this work shows a success in producing the dynamical properties of a galaxy it highlights how much is left to be done. The Tully-Fisher relation seems to indicate that there is a physical connection between the dark matter component and the baryonic component in spiral galaxies.

For these HI-selected galaxies, many of which are dwarfs or irregulars rather than spirals, we find less of a correlation between  $V_{rot}$  or  $M_{dyn}$  and  $M_{bar}$  than is usually found for spiral galaxies (e.g., Giovanelli et al. 1997) culling out the systems with axis ratios greater than or equal to 0.4. However, even for this disparate group of galaxies, the average surface density of gas (Rosenberg & Schneider 2003) has a very small range relative to the variation in the stellar surface density. The surface density of the gas is determined as the HI mass divided by

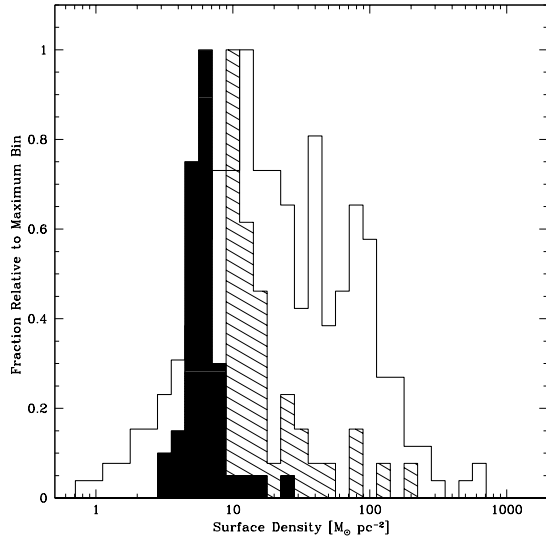


FIG. 9.— The distribution of mass surface densities of gas, stars, and baryons. The gas surface densities, indicated by the dark-shaded histogram, come from the RS sample galaxies with measured HI sizes. The open histogram shows the stellar mass surface densities of the RS and SS galaxies using the J-band luminosity to estimate stellar mass, and the J-band sizes. The total baryonic mass surface density (cross-hatched histogram) is estimated using the sum of gas and stars and the optical size of each galaxy.

the HI area defined by the size at  $2 \times 10^{20} \text{ cm}^{-2}$ .

Figure 9 shows the HI surface densities for the RS galaxies with measured HI sizes. Rosenberg & Schneider (2003) showed that the average surface density of the gas in these galaxies was nearly constant, and this result is evident in the small range in mean HI surface densities: the values range from 3 to  $24 \text{ M}_{\odot} \text{ pc}^{-2}$  with only 4 of the 50 galaxies having values above 10. We do not discuss the surface densities of the SS sample because HI sizes are not available for these galaxies. Alternatively, the stellar surface densities or the RS and SS sample cover a broad distribution ranging from 0.8 to  $660 \text{ M}_{\odot} \text{ pc}^{-2}$ . The notable feature of this plot is that the dispersion in the HI surface density is only 0.46 while the dispersion around the stellar mass surface density is 4.5. The baryonic mass surface density is the combination of the HI and stellar masses as given in Equation 2 and has a standard deviation around the mean surface density (averaged over the HI size) of 5.8. These mass surface densities may provide an additional constraint for the simulations.

The larger dispersion in the stellar mass surface density of the RS and SS samples is, at least in part, due to the large uncertainties in the J-band sizes. Also, since the diameters were measured at a high surface brightness, the mean surface densities are higher than they would have been had we measured out to an equivalently low surface density as the gas. The median value for the distribution is  $19.3 \text{ M}_{\odot} \text{ pc}^{-2}$  relative to  $5.9 \text{ M}_{\odot} \text{ pc}^{-2}$  for the HI mass density. We note that the median value of the mass surface density is generally higher for the stars than for the gas. This corresponds well with the observation that many gas-rich galaxies have gas distributions extending well beyond the optical (or near infrared) light distributions. However, we do note that there are still some systems in the sample that have very low stellar

mass surface densities providing an indication that we have detected some very low surface brightness systems.

## 5. THE MORPHOLOGY OF HI-SELECTED GALAXIES

Figures 1 and 3 in the Appendix show the 2MASS J-band images for the RS and SS galaxies with measured values of baryonic mass, respectively. The galaxies have been placed in order of their baryonic mass from the highest baryonic mass systems to the lowest (within each survey). Figures 2 and 4 show the galaxies for which we do not measure baryonic mass.

The images of these galaxies illustrate the diverse population as discussed in §3. The sample covers the range from nearby bright spiral galaxies like RS 189, NGC 4565, to bulge-less low surface brightness smudges like RS 184 (Figure 1 in the middle of the second to last line on the second page). There are also early type galaxies in the sample like SS 19 (Figure 3 in the middle of the last line) which is NGC 7712, an elliptical galaxy (Scodeggio et al. 1995) and close interacting pairs like RS 50 (second to last image in Figure 2).

The SS98 optical images of the SS sample indicate that a substantial fraction of the galaxies are low surface brightness. As discussed in §3, these 2MASS data also indicate that there is a substantial population of low surface brightness galaxies among the RS and SS samples even though the surface brightness can not be directly compared with the usual low surface brightness definition. Comparing the 2MASS images with the SS98 optical images, we find that nearly all of the low surface brightness galaxies are not detected or are barely detected in the 2MASS data. Inevitably this is because 2MASS is a shallow survey, but there is no evidence for bulges that are bright in the infrared but not in the optical as was found for low surface brightness galaxies by Galaz et al. (2002).

Visual inspection of the RS galaxy images seems to indicate that most of the highest baryonic mass galaxies are spirals with prominent bulge components while the lower baryonic mass galaxies show more variation galaxy type and bulge size down to galaxies like RS 184 where the brightness distribution appears fairly flat across the J-band detected stellar disk. This same trend is not apparent for the SS galaxies, but the sample size is significantly smaller which might account for the difference.

## 6. SUMMARY

We have examined the stellar properties of two HI-selected galaxy samples and found that they show a large range of stellar properties. We find that the galaxies cover a wide range in mass-to-luminosity ratio and the ratio is uncorrelated with the HI mass of the system. The range suggests that star formation does not proceed uniformly in all galaxies, some of the galaxies have funneled a large fraction of their gas mass into stars by the present day while there are other galaxies that are still largely dominated by their gas content. Because of these differences, one cannot infer the gas properties of a galaxy from its stellar properties and vice versa. The different proportions of gas and stars in these galaxies may be providing us a glimpse of galaxies in different stages of evolution.

Despite the wide range of gas-to-star ratios for galaxies in these samples, there are some surprising correlations.

There is a small range in the average HI surface density in these galaxies. While the average stellar surface density distribution is not as tight, it is also a fairly narrow distribution given all of the inaccuracies in its measurement. The baryonic matter appears to average to about one quarter of the dynamical mass (within the optical dimensions of the galaxy) across a wide range of galaxy types.

Most notably, the size of the stellar disk appears to be a very good predictor of the total baryonic content of galaxies. The physical causes of this correlation are not immediately apparent, but the correlation spans over three orders of magnitude in galaxy mass.

We would like to thank 2MASS for the effort that has gone into this catalog and for providing financial support for this research. We would particularly like to thank Roc

Cutri for all of the help in obtaining the full resolution images that were needed for this paper to be possible. We would also like to thank the Arecibo and VLA staffs for their assistance with the HI observations. Thanks also to Eric Bell for the information on J-band M/L ratios. We also appreciate John Spitzak's work on the program to display and print the galaxy images. Thanks also go to the anonymous referee for helpful suggestions. JLR acknowledges support from the National Science Foundation under grant AST-0302049. The Digitized Sky Surveys were produced at the Space Telescope Science Institute under U.S. Government grant NAG W-2166. The images of these surveys are based on photographic data obtained using the Oschin Schmidt Telescope on Palomar Mountain and the UK Schmidt Telescope. The plates were processed into the present compressed digital form with the permission of these institutions.

## APPENDIX

In this appendix we present the 2MASS data for the HI-selected samples. The data include tables of the 2MASS size and magnitude values which are presented since many of these values are measured from the images themselves or are derived from the Version 2 extended source catalogs which are not generally available. The information in Table 1, the ADBS data, is as follows: (1) the sequential listing in the RS catalog; (2) the name from the ADBS catalog; (3, 4) the RA and DEC from the HI catalog, (5,6) the RA and DEC from the 2MASS catalog if it was identified or of the 2MASS image center, (7) the radius of the 21 mag arcsec<sup>-2</sup> isophote; (8) the b/a axis ratio used to measure the magnitude within the 21 mag arcsec<sup>-2</sup> isophote; (9) J 21 mag arcsec<sup>-2</sup> isophotal magnitude ( $J_{21}$ ); (10) Error in  $J_{21}$ , (11) the radius used for the aperture magnitude; (12) J-band aperture magnitude; (13) error in the J-band aperture magnitude; (14) method used for determining the magnitudes – V2 and V3 refer to sources measured from the Version 2 or 3 catalog, MI are sources measured off the images, and NM are sources for which there was nothing on the 2MASS images to measure. The data in Table 2, the SS data, are the same except that the SS catalog name and the sequential catalog number are the same so all columns starting from the RA and DEC from the HI catalog are shifted one to the left.

The images are presented as a quick look at the galaxies in the sample. The objects have been placed in order of baryonic mass from the most massive to the least massive. Objects in Figures 2 and 4 are sources for which a baryonic mass was not determined.



## REFERENCES

- Allen C. W., 1973, *Astrophysical Quantities*, 3rd edn. Athlone Press, London.
- Bell, E. F. & de Jong, R. S. 2001, *ApJ*, 550, 212.
- Cole, S., Norberg, P., Baugh, C. M., Frenk, C. S., Bland-Hawthorn, J., Bridges, T., Cannon, R., Colless, M., Collins, C., Couch, W., Cross, N., Dalton, G., De Propris, R., Driver, S. P., Efstathiou, G., Ellis, R. S., Glazebrook, K., Jackson, C., Lahav, O., Lewis, I., Lumsden, S., Maddox, S., Madgwick, D., Peacock, J. A., Peterson, B. A., Sutherland, W., Taylor, K. 2001, *MNRAS*, 326, 255.
- Fisher, J. R. & Tully, R. B. 1981, *ApJ*, 243, L23.
- Galaz, G., Dalcanton, J. J., Infante, L. & Triester, E. 2002, *ApJ*, 124, 1360.
- Governato, F., Mayer, L., Wadsley, J., Gardner, J. P., Willman, B., Hayashi, E., Quinn, T., Stadel, J., & Lake, G. 2004, *ApJ*, 607, 688.
- Huchtmeier, W. K. & Richter, O. -G. 1985, *A&AS*, 149, 118.
- Johnson H. L., 1966, *ARA&A*, 4, 193.
- Kennicutt, R. C. Jr. 1998, *ApJ*, 498, 541.
- McGaugh, S. S., Schombert J. M., Bothun, G. D., & de Blok, W. J. G. 2000, *ApJ*, 533, 102.
- McGaugh, S. S. & de Blok, W. J. G. 1997, *ApJ*, 481, 689.
- Meyer, M. J., Zwaan, M. A., Webster, R. L., Smith, L., Ryan-Weber, E., Drinkwater, M. J., Barnes, D. G., Howlett, M., Kilborn, V. A., Stevens, J., Waugh, M., Pierce, M. J., Bhathal, R., de Blok, W. J. G., Disney, M. J., Ekers, R. D., Freeman, K. C., Garcia, D. A., Gibson, B. K., Harnett, J., Henning, P. A., Jerjen, H., Kesteven, M. J., Knezek, P. M., Koribalski, B. S., Mader, S., Marquarding, M., Minchin, R. F., O'Brien, J., Oosterloo, T., Price, R. M., Putman, M. E., Ryder, S. D., Sadler, E. M., Stewart, I. M., Stootman, F., Wright, A. E. 2004, *MNRAS*, 350, 1195.
- Mo, H. J. & Mao, S. 2000, *MNRAS*, 318, 163.
- O'Neil, K., Bothun, G. D., & Schombert, J. 2000, *AJ*, 119, 136.
- Rosenberg, J. L. & Schneider, S. E. 2003, *ApJ*, 585, 256.
- Rosenberg, J. L. & Schneider, S. E. 2002, *ApJ*, 567, 247.
- Rosenberg, J. L. & Schneider, S. E. 2000, *ApJS*, 130, 177 [RS00].
- Scodreggio, M. & Gavazzi, G. 1993, *ApJ*, 409, 110.
- Scodreggio, M., Solanes, J. M., Giovanelli, R., & Haynes, M. P. 1995, *ApJ*, 444, 41.
- Spitzak, J. G. & Schneider, S. E. 1998, *ApJS*, 119, 159 [SS98].
- Shen, S., Mo, H. J., & Shu, C. 2002, *MNRAS*, 331, 259.
- Sprayberry, D., Impey, C. D., Bothun, G. D., & Irwin, M. J. 1995, *AJ*, 109, 558.
- Wevers, B. M. H. R., van der Kruit, P. C., & Allen, R. J., 1986, *A&SS*, 66, 505.
- Zavala, J., Avila-Reese, V., Hernández-Toledo, H., Firmani, C. 2003, *A&A*, 412, 633.
- Zwaan, M., Briggs, F. H., Sprayberry, D. & Sorar, E. 1997, *ApJ*, 490, 173.

Table 1. 2MASS Data for ADBS Galaxies

| ADBS<br>Num. | ADBS<br>Name | $\alpha_{ADBS}$<br>deg | $\delta_{ADBS}$<br>deg | $\alpha_{2MASS}$<br>deg | $\delta_{2MASS}$<br>deg | R <sub>J21e</sub><br>" | b/a <sub>J21</sub> | J <sub>21e</sub> | err <sub>J21e</sub> | R <sub>Aper</sub><br>" | J <sub>Aper</sub> | err <sub>JAp</sub> | Method. |
|--------------|--------------|------------------------|------------------------|-------------------------|-------------------------|------------------------|--------------------|------------------|---------------------|------------------------|-------------------|--------------------|---------|
| rs001        | 000330+2312  | 0.8957                 | 23.2011                | 0.895847                | 23.200817               | 20.2                   | 0.58               | 12.189           | 0.031               | 50.0                   | 11.644            | 0.050              | V3      |
| rs002        | 000407+2234  | 1.0292                 | 22.5820                | ...                     | ...                     | ...                    | ...                | ...              | ...                 | 30.0                   | 13.436            | 0.111              | MI      |
| rs003        | 000623+2347  | 1.5949                 | 23.7891                | 1.595224                | 23.789404               | 14.2                   | 0.36               | 14.347           | 0.085               | 25.0                   | 13.661            | 0.125              | V3      |
| rs004        | 000900+2348  | 2.2269                 | 23.8176                | 2.227971                | 23.816923               | 19.4                   | 0.50               | 12.969           | 0.050               | 25.0                   | 12.729            | 0.055              | V3      |
| rs005        | 001622+2237  | 4.0929                 | 22.6170                | 4.093417                | 22.616209               | 13.4                   | 0.42               | 13.609           | 0.046               | 25.0                   | 13.371            | 0.089              | V3      |
| rs006        | 002249+2310  | 5.6894                 | 23.1953                | 5.689276                | 23.195107               | 8.0                    | 0.82               | 14.265           | 0.067               | 25.0                   | 13.492            | 0.107              | V3      |
| rs007        | 002526+2136  | 6.3600                 | 21.6040                | 6.361917                | 21.603350               | ...                    | ...                | ...              | ...                 | 15.0                   | 14.9              | ...                | MI      |
| rs008        | 003426+2436  | 8.6108                 | 24.6010                | 8.603510                | 24.603650               | 2.9                    | 1.0                | 17.1             | ...                 | 15.0                   | 15.1              | ...                | MI      |
| rs009        | 003751+0838  | 9.4905                 | 8.6348                 | 9.490385                | 8.635223                | 36.7                   | 0.7                | 10.821           | 0.025               | 70.0                   | 10.432            | 0.029              | V3      |
| rs010        | 003811+2523  | 9.5458                 | 25.3960                | 9.548830                | 25.395960               | 8.1                    | 0.5                | 15.5             | ...                 | 20.0                   | 14.7              | ...                | MI      |
| rs011        | 004649+2134  | 11.7042                | 21.5830                | ...                     | ...                     | 2.8                    | 1.0                | 17.1             | ...                 | 7.0                    | 17.0              | ...                | MI      |
| rs012        | 011440+2708  | 18.6679                | 27.1350                | 18.690270               | 27.135980               | ...                    | ...                | ...              | ...                 | 15.0                   | 15.1              | ...                | MI      |
| rs013        | 014206+1235  | 25.5397                | 12.6008                | 25.540237               | 12.601927               | 32.4                   | 0.56               | 10.952           | 0.021               | 60.0                   | 10.740            | 0.032              | V3      |
| rs014        | 014246+1309  | 25.6950                | 13.1550                | ...                     | ...                     | 28.8                   | 0.44               | 12.5610          | 0.036               | 70.0                   | 11.954            | 0.075              | V2      |
| rs015        | 014527+2531  | 26.3650                | 25.5220                | ...                     | ...                     | 7.0                    | 1.0                | 15.7930          | 0.228               | 60.0                   | 12.936            | 0.140              | V2      |
| rs016        | 014729+2719  | 26.8757                | 27.3316                | 26.874540               | 27.333349               | ...                    | ...                | ...              | ...                 | 115.0 <sup>1</sup>     | 11.069            | 0.056              | V3      |
| rs017        | 014847+1034  | 27.1958                | 10.5690                | 27.218527               | 10.589932               | 30.2                   | 0.34               | 11.793           | 0.025               | 30.0                   | 11.690            | 0.025              | V3      |
| rs018        | 015011+2309  | 27.5492                | 23.1560                | 27.555040               | 23.159340               | 4.6                    | 0.9                | 15.8             | ...                 | 20.0                   | 12.6              | ...                | MI      |
| rs019        | 015105+1235  | 27.7721                | 12.5880                | ...                     | ...                     | ...                    | ...                | ...              | ...                 | 30.0                   | 13.869            | 0.130              | MI      |
| rs020        | 015434+2312  | 28.6429                | 23.2040                | 28.642710               | 23.204920               | 3.8                    | 0.9                | 17.1             | ...                 | 20.0                   | 15.0              | ...                | MI      |
| rs021        | 015443+1033  | 28.6800                | 10.5660                | 28.692800               | 10.563700               | ...                    | ...                | ...              | ...                 | ...                    | ...               | ...                | NM      |
| rs022        | 015906+2523  | 29.7888                | 25.3855                | 29.789383               | 25.385777               | 14.8                   | 0.50               | 13.838           | 0.066               | 50.0                   | 12.255            | 0.078              | V3      |
| rs023        | 020022+2434  | 30.0972                | 24.5805                | 30.097410               | 24.580576               | 24.7                   | 0.76               | 11.816           | 0.029               | 60.0                   | 11.461            | 0.050              | V3      |
| rs024        | 020045+2809  | 30.1883                | 28.1660                | 30.188300               | 28.166000               | ...                    | ...                | ...              | ...                 | ...                    | ...               | ...                | NM      |
| rs025        | 020148+2632  | 30.4430                | 26.5466                | 30.443739               | 26.546976               | 20.7                   | 0.48               | 12.013           | 0.023               | 30.0                   | 11.895            | 0.029              | V3      |
| rs026        | 020320+1837  | 30.8342                | 18.6295                | 30.834126               | 18.629620               | 18.6                   | 1.0                | 12.775           | 0.048               | 50.0                   | 12.294            | 0.080              | V3      |
| rs027        | 020320+2345  | 30.8371                | 23.7610                | 30.837140               | 23.76093                | 5.8                    | 1.0                | 15.9             | ...                 | 30.0                   | 14.2              | ...                | MI      |
| rs028        | 020405+2412  | 31.0208                | 24.2090                | ...                     | ...                     | ...                    | ...                | ...              | ...                 | 70.0                   | 12.412            | 0.093              | V2      |
| rs029        | 020918+2534  | 32.3093                | 25.5706                | 32.309147               | 25.570778               | 20.8                   | 0.52               | 11.803           | 0.021               | 40.0                   | 11.521            | 0.031              | V3      |
| rs030        | 022807+1935  | 37.0462                | 19.5996                | 37.046249               | 19.599314               | 52.6                   | 0.54               | 10.387           | 0.008               | 95.2 <sup>1</sup>      | 10.288            | 0.026              | V2      |
| rs031        | 022859+2808  | 37.2458                | 28.1450                | ...                     | ...                     | ...                    | ...                | ...              | ...                 | 30.0                   | 14.352            | 0.223              | MI      |
| rs032        | 023322+2034  | 38.3442                | 20.5820                | ...                     | ...                     | ...                    | ...                | ...              | ...                 | 30.0                   | 13.955            | 0.185              | MI      |
| rs033        | 023323+2810  | 38.3479                | 28.1790                | 38.317542               | 28.178069               | ...                    | ...                | ...              | ...                 | ...                    | ...               | ...                | NM      |
| rs034        | 023432+2234  | 38.6358                | 22.5760                | ...                     | ...                     | 4.6                    | 1.0                | 18.6             | ...                 | ...                    | ...               | ...                | NM      |
| rs035        | 023622+2526  | 39.0677                | 25.4238                | 39.067299               | 25.423820               | 38.8                   | 0.4                | 11.651           | 0.017               | 135.1 <sup>1</sup>     | 10.844            | 0.033              | V2      |
| rs036        | 024328+2035  | 40.8671                | 20.5960                | ...                     | ...                     | 7.0                    | 0.94               | 14.639           | 0.070               | 20.0                   | 13.743            | 0.090              | V2      |
| rs037        | 025537+1938  | 43.9071                | 19.6340                | ...                     | ...                     | 2.0                    | 1.0                | 17.6             | ...                 | ...                    | ...               | ...                | NM      |
| rs038        | 025726+1008  | 44.3608                | 10.1380                | 44.362360               | 10.431630               | 5.5                    | 1.0                | 15.9             | ...                 | 40.0                   | 13.2              | ...                | MI      |
| rs039        | 025749+1110  | 44.4740                | 11.1831                | 44.473911               | 11.182944               | 25.5                   | 0.70               | 12.134           | 0.041               | 60.0                   | 11.772            | 0.073              | V3      |
| rs040        | 025942+2514  | 44.9245                | 25.2371                | 44.928493               | 25.241194               | 60.8                   | 0.48               | 10.396           | 0.019               | 70.0                   | 10.004            | 0.015              | V3      |
| rs041        | 030525+0835  | 46.3550                | 8.5870                 | ...                     | ...                     | 7.0                    | 0.52               | 16.043           | 0.190               | 30.0                   | 14.170            | 0.201              | V2      |
| rs042        | 030546+2212  | 46.4450                | 22.2036                | 46.444927               | 22.203434               | 19.4                   | 0.56               | 12.520           | 0.033               | 30.0                   | 12.293            | 0.041              | V3      |
| rs043        | 031420+2409  | 48.5824                | 24.1539                | 48.582500               | 24.153975               | 9.5                    | 0.68               | 14.462           | 0.073               | 25.0                   | 13.869            | 0.132              | V3      |
| rs044        | 032327+1109  | 50.8505                | 11.1527                | 50.850002               | 11.152466               | 21.2                   | 0.18               | 14.116           | 0.073               | 25.0                   | 13.581            | 0.115              | V3      |
| rs045        | 033112+1410  | 52.7762                | 14.1770                | 52.776714               | 14.177110               | 18.8                   | 0.44               | 13.081           | 0.046               | 30.0                   | 12.849            | 0.071              | V3      |
| rs046        | 034444+0833  | 56.1920                | 8.5627                 | 56.191986               | 8.562414                | 13.1                   | 0.54               | 13.962           | 0.078               | 40.0                   | 12.996            | 0.133              | V3      |
| rs047        | 033456+1507  | 53.7034                | 15.1421                | 53.703297               | 15.141906               | 12.9                   | 0.30               | 14.726           | 0.084               | 20.0                   | 14.358            | 0.168              | V3      |
| rs048        | 040325+2034  | 60.8550                | 20.5770                | ...                     | ...                     | ...                    | ...                | ...              | ...                 | 30.0                   | 14.064            | 0.183              | MI      |
| rs049        | 040344+2209  | 60.9339                | 22.1582                | 60.933250               | 22.159042               | 29.2                   | 0.80               | 10.836           | 0.020               | 60.0                   | 10.673            | 0.029              | V3      |
| rs050        | 040411+2207  | 61.0405                | 22.1309                | 61.040314               | 22.131767               | ...                    | ...                | ...              | ...                 | ...                    | ...               | ...                | NM      |

Table 1—Continued

| ADBS<br>Num. | ADBS<br>Name | $\alpha_{ADBS}$<br>deg | $\delta_{ADBS}$<br>deg | $\alpha_{MASS}$<br>deg | $\delta_{MASS}$<br>deg | $R_{J21e}$<br>" | b/a <sub>J21</sub> | J <sub>21e</sub> | err <sub>J21e</sub> | $R_{Aper}$<br>" | J <sub>Aper</sub> | err <sub>J<sub>Ap</sub></sub> | Method. |
|--------------|--------------|------------------------|------------------------|------------------------|------------------------|-----------------|--------------------|------------------|---------------------|-----------------|-------------------|-------------------------------|---------|
| rs051        | 040731+2210  | 61.8829                | 22.1690                | 61.885460              | 22.167440              | 11.8            | 1.0                | 12.0             | ...                 | 15.0            | 11.7              | ...                           | MI      |
| rs052        | 041255+1328  | 63.2051                | 13.4961                | 63.205006              | 13.495862              | 14.2            | 0.84               | 12.613           | 0.033               | 30.0            | 12.313            | 0.042                         | V3      |
| rs053        | 041336+2528  | 63.4121                | 25.4829                | 63.411591              | 25.482941              | 49.7            | 0.28               | 10.815           | 0.016               | 50.0            | 10.682            | 0.017                         | V3      |
| rs054        | 043622+1309  | 69.0929                | 13.1600                | ...                    | ...                    | ...             | ...                | ...              | ...                 | 30.0            | 13.520            | 0.125                         | MI      |
| rs055        | 043649+2409  | 69.2112                | 24.1522                | 69.210838              | 24.152411              | 12.8            | 0.38               | 14.393           | 0.086               | 25.0            | 13.698            | 0.138                         | V3      |
| rs056        | 044310+1010  | 70.7942                | 10.1720                | ...                    | ...                    | 2.8             | 1.0                | 18.5             | ...                 | ...             | ...               | ...                           | NM      |
| rs057        | 044753+2346  | 71.9729                | 23.7800                | ...                    | ...                    | 3.0             | 1.0                | 18.4             | ...                 | ...             | ...               | ...                           | NM      |
| rs058        | 045254+2310  | 73.2258                | 23.1810                | 73.220940              | 23.166440              | 4.1             | 1.0                | 16.8             | ...                 | 40.0            | 13.1              | ...                           | MI      |
| rs059        | 051733+1934  | 79.4228                | 19.6000                | 79.422737              | 19.600281              | 30.1            | 0.22               | 12.553           | 0.033               | 30.0            | 12.470            | 0.048                         | V3      |
| rs060        | 053017+2233  | 82.5729                | 22.5660                | ...                    | ...                    | ...             | ...                | ...              | ...                 | ...             | ...               | ...                           | NM      |
| rs061        | 053522+1332  | 83.8186                | 13.5489                | 83.818535              | 13.548637              | 19.9            | 0.32               | 12.950           | 0.030               | 30.0            | 12.783            | 0.054                         | V3      |
| rs062        | 053844+1508  | 84.6671                | 15.1475                | 84.667244              | 15.147024              | 28.5            | 0.44               | 11.615           | 0.026               | 40.0            | 11.322            | 0.029                         | V3      |
| rs063        | 055452+1509  | 88.6697                | 15.1712                | 88.669701              | 15.170404              | 24.9            | 0.46               | 12.295           | 0.034               | 60.0            | 11.793            | 0.070                         | V3      |
| rs064        | 055517+2526  | 88.8221                | 25.4430                | 88.825625              | 25.442286              | ...             | ...                | ...              | ...                 | ...             | ...               | ...                           | NM      |
| rs065        | 060719+1936  | 91.8292                | 19.6030                | 91.831590              | 19.601240              | 8.5             | 0.7                | 14.550           | ...                 | 25.0            | 13.7              | ...                           | MI      |
| rs066        | 060733+0932  | 91.8892                | 9.5360                 | ...                    | ...                    | 5.0             | 1.0                | 15.9             | ...                 | ...             | ...               | ...                           | NM      |
| rs067        | 061543+1110  | 93.9292                | 11.1670                | 93.937620              | 11.172750              | 10.0            | 0.4                | 14.3             | ...                 | 25.0            | 13.3              | ...                           | MI      |
| rs068        | 061729+2807  | 94.3552                | 28.1212                | 94.355087              | 28.121138              | 18.7            | 0.54               | 12.968           | 0.043               | 50.0            | 12.351            | 0.082                         | V3      |
| rs069        | 062054+2008  | 95.2271                | 20.1410                | 95.263125              | 20.170111              | ...             | ...                | ...              | ...                 | 15.0            | 15.4              | ...                           | MI      |
| rs070        | 062103+2010  | 95.2629                | 20.1700                | ...                    | ...                    | 2.1             | 1.0                | 17.9             | ...                 | ...             | ...               | ...                           | NM      |
| rs071        | 062302+1108  | 95.7424                | 11.1417                | 95.742302              | 11.142012              | 45.1            | 0.36               | 12.414           | 0.087               | 40.0            | 12.216            | 0.078                         | V3      |
| rs072        | 063549+1107  | 98.9550                | 11.1280                | 98.977410              | 11.136020              | 21.0            | 0.7                | 8.650            | ...                 | ...             | ...               | ...                           | NM      |
| rs073        | 063603+1109  | 99.0142                | 11.1520                | 98.975083              | 11.134497              | ...             | ...                | ...              | ...                 | ...             | ...               | ...                           | NM      |
| rs074        | 065008+2009  | 102.5622               | 20.1409                | 102.561920             | 20.140766              | 22.5            | 0.66               | 11.479           | 0.020               | 40.0            | 11.123            | 0.021                         | V3      |
| rs075        | 065406+0834  | 103.5258               | 8.5720                 | 103.523490             | 8.571820               | 6.7             | 0.4                | 16.1             | ...                 | 20.0            | 14.8              | ...                           | MI      |
| rs076        | 065718+1332  | 104.3250               | 13.5363                | 104.312889             | 13.539122              | 7.0             | 0.76               | 14.853           | 0.079               | 30.0            | 13.399            | 0.102                         | V2      |
| rs077        | 070911+2036  | 107.3001               | 20.6023                | 107.299553             | 20.602835              | 20.9            | 0.76               | 11.350           | 0.019               | 40.0            | 11.131            | 0.023                         | V3      |
| rs078        | 071028+2307  | 107.6204               | 23.1320                | ...                    | ...                    | 4.1             | 1.0                | 18.3             | ...                 | ...             | ...               | ...                           | NM      |
| rs079        | 071225+2342  | 108.1043               | 23.7124                | 108.104881             | 23.711788              | ...             | ...                | ...              | ...                 | 30.0            | 12.935            | 0.083                         | NM      |
| rs080        | 071352+1031  | 108.4671               | 10.5240                | ...                    | ...                    | 9.6             | 0.1                | 16.637           | 0.257               | 70.0            | 12.111            | 0.083                         | V2      |
| rs081        | 071553+1207  | 108.9721               | 12.1170                | 108.969116             | 12.115514              | 7.0             | 1.0                | 15.159           | 0.209               | 60.0            | 12.749            | 0.134                         | V2      |
| rs082        | 071831+2709  | 109.6334               | 27.1584                | 109.632622             | 27.157993              | 29.8            | 0.22               | 12.576           | 0.040               | 30.0            | 12.478            | 0.058                         | V3      |
| rs083        | 072502+2348  | 111.2564               | 23.7832                | 111.256935             | 23.783270              | 32.3            | 0.54               | 11.088           | 0.019               | 50.0            | 11.002            | 0.021                         | V3      |
| rs084        | 072507+0931  | 111.2931               | 9.5160                 | 111.293152             | 9.515792               | 24.0            | 0.60               | 12.115           | 0.048               | 40.0            | 11.803            | 0.057                         | V3      |
| rs085        | 072858+2035  | 112.2254               | 20.5911                | 112.225601             | 20.591793              | 32.1            | 0.40               | 11.712           | 0.027               | 50.0            | 11.472            | 0.040                         | V3      |
| rs086        | 073445+2234  | 113.7050               | 22.5765                | 113.704926             | 22.576496              | 10.6            | 0.60               | 14.447           | 0.075               | 25.0            | 13.604            | 0.101                         | V3      |
| rs087        | 073533+1131  | 113.8908               | 11.5190                | ...                    | ...                    | 7.0             | 1.0                | 15.651           | 0.219               | 50.0            | 13.096            | 0.147                         | V2      |
| rs088        | 081538+2107  | 123.9100               | 21.1310                | 123.932500             | 21.131500              | 4.9             | 1.0                | 15.8             | ...                 | 15.0            | 15.1              | ...                           | MI      |
| rs089        | 081617+2308  | 124.0729               | 23.1391                | ...                    | ...                    | 7.0             | 1.0                | 15.582           | 0.154               | 50.0            | 14.400            | 0.369                         | V2      |
| rs090        | 081707+2433  | 124.2808               | 24.5640                | 124.282700             | 24.562860              | 2.6             | 1.0                | 17.300           | ...                 | 10.0            | 15.6              | ...                           | MI      |
| rs091        | 081726+2110  | 124.3560               | 21.1637                | 124.355927             | 21.163906              | 11.9            | 0.54               | 14.545           | 0.087               | 30.0            | 13.757            | 0.148                         | V3      |
| rs092        | 081821+2431  | 124.5822               | 24.5269                | 124.582169             | 24.526777              | 7.0             | 0.82               | 14.309           | 0.058               | 25.0            | 13.883            | 0.147                         | V3      |
| rs093        | 081904+2111  | 124.7577               | 21.1859                | 124.757904             | 21.185919              | 21.8            | 0.84               | 12.259           | 0.037               | 60.0            | 11.805            | 0.065                         | V3      |
| rs094        | 081915+2030  | 124.8034               | 20.5109                | 124.803284             | 20.510710              | 32.5            | 0.64               | 11.006           | 0.019               | 60.0            | 10.729            | 0.025                         | V3      |
| rs095        | 081926+2345  | 124.8433               | 23.7472                | 124.843201             | 23.747368              | 10.3            | 0.60               | 14.149           | 0.062               | 25.0            | 13.757            | 0.124                         | V3      |
| rs096        | 082430+1835  | 126.1290               | 18.5969                | 126.129059             | 18.597067              | 20.1            | 0.72               | 12.287           | 0.030               | 40.0            | 11.978            | 0.041                         | V3      |
| rs097        | 082551+2807  | 126.4484               | 28.1182                | 126.448250             | 28.118372              | 22.0            | 0.26               | 13.699           | 0.067               | 25.0            | 13.405            | 0.096                         | V3      |
| rs098        | 083209+2233  | 128.0474               | 22.5606                | 128.047058             | 22.560581              | 26.3            | 0.88               | 10.525           | 0.015               | 60.0            | 10.196            | 0.018                         | V3      |
| rs099        | 084025+1834  | 130.1058               | 18.5670                | 130.113270             | 18.573810              | 4.6             | 0.4                | 17.200           | ...                 | 30.0            | 14.1              | ...                           | MI      |
| rs100        | 084316+1305  | 130.8162               | 13.0858                | 130.816666             | 13.085848              | 32.0            | 0.30               | 12.215           | 0.038               | 40.0            | 11.940            | 0.051                         | V3      |

Table 1—Continued

| ADBS<br>Num. | ADBS<br>Name | $\alpha_{ADBS}$<br>deg | $\delta_{ADBS}$<br>deg | $\alpha_{2MASS}$<br>deg | $\delta_{2MASS}$<br>deg | $R_{J21e}$<br>" | b/a <sub>J21</sub> | J <sub>21e</sub> | err <sub>J21e</sub> | $R_{Aper}$<br>" | J <sub>Aper</sub> | err <sub>JAp</sub> | Method. |
|--------------|--------------|------------------------|------------------------|-------------------------|-------------------------|-----------------|--------------------|------------------|---------------------|-----------------|-------------------|--------------------|---------|
| rs101        | 084411+2208  | 131.0581               | 22.1369                | 131.057724              | 22.136482               | 7.5             | 0.74               | 14.726           | 0.100               | 25.0            | 14.089            | 0.221              | V3      |
| rs102        | 084427+0930  | 131.0918               | 9.5376                 | 131.090469              | 9.537537                | 11.4            | 0.28               | 14.997           | 0.087               | 20.0            | 14.421            | 0.179              | V3      |
| rs103        | 084504+0932  | 131.2675               | 9.5400                 | 131.281586              | 9.541821                | ...             | ...                | ...              | ...                 | 15.0            | 15.552            | 0.344              | V2      |
| rs104        | 084743+1325  | 131.9239               | 13.4189                | 131.923630              | 13.419150               | 15.9            | 0.94               | 12.221           | 0.033               | 30.0            | 11.973            | 0.036              | V3      |
| rs105        | 084804+2519  | 132.0171               | 25.3320                | 132.014470              | 25.332790               | 3.8             | 0.6                | 17.3             | ...                 | 7.0             | 16.4              | ...                | MI      |
| rs106        | 085751+1230  | 134.4658               | 12.5020                | 134.469040              | 12.495370               | 7.5             | 1.0                | 14.9             | ...                 | 20.0            | 14.2              | ...                | MI      |
| rs107        | 085927+1108  | 134.8650               | 11.1390                | 134.847916              | 11.135059               | 9.6             | 0.72               | 14.661           | 0.091               | 25.0            | 13.982            | 0.146              | V2      |
| rs108        | 085953+2109  | 134.9744               | 21.1518                | 134.974915              | 21.151529               | 8.9             | 0.54               | 14.782           | 0.076               | 25.0            | 13.940            | 0.138              | V3      |
| rs109        | 090024+2536  | 135.1000               | 25.6130                | 135.098663              | 25.612085               | 18.8            | 0.86               | 14.247           | 0.076               | 60.0            | 12.740            | 0.106              | V2      |
| rs110        | 090102+1105  | 135.2631               | 11.0977                | 135.263443              | 11.098387               | 18.0            | 0.84               | 12.473           | 0.049               | 30.0            | 12.302            | 0.056              | V3      |
| rs111        | 090129+2110  | 135.3666               | 21.1755                | 135.365799              | 21.175022               | 9.9             | 0.74               | 14.305           | 0.071               | 25.0            | 13.744            | 0.118              | V3      |
| rs112        | 090143+1105  | 135.4207               | 11.0829                | 135.420670              | 11.082906               | 16.2            | 0.68               | 12.861           | 0.053               | 40.0            | 12.514            | 0.097              | V3      |
| rs113        | 090240+1306  | 135.6728               | 13.1074                | 135.672501              | 13.107930               | 16.0            | 0.38               | 13.544           | 0.049               | 30.0            | 13.351            | 0.108              | V3      |
| rs114        | 090526+2533  | 136.3597               | 25.5504                | 136.359344              | 25.551037               | 12.8            | 0.48               | 14.261           | 0.070               | 30.0            | 13.448            | 0.109              | V3      |
| rs115        | 090544+2532  | 136.4371               | 25.5390                | 136.437083              | 25.539000               | ...             | ...                | ...              | ...                 | ...             | ...               | ...                | NM      |
| rs116        | 090548+2526  | 136.4496               | 25.4373                | 136.449554              | 25.437365               | 28.8            | 0.64               | 11.357           | 0.020               | 70.0            | 10.489            | 0.024              | V3      |
| rs117        | 090552+2520  | 136.4692               | 25.3440                | 136.469167              | 25.344000               | ...             | ...                | ...              | ...                 | 7.0             | 16.6              | ...                | MI      |
| rs118        | 093314+2307  | 143.3181               | 23.1348                | 143.318192              | 23.134792               | 14.6            | 0.68               | 13.295           | 0.049               | 40.0            | 12.719            | 0.086              | V3      |
| rs119        | 093704+0932  | 144.2599               | 9.5403                 | 144.259537              | 9.539845                | 13.7            | 0.32               | 14.009           | 0.073               | 25.0            | 13.454            | 0.128              | V3      |
| rs120        | 093805+0931  | 144.5335               | 9.5231                 | 144.532791              | 9.523837                | 46.7            | 0.32               | 10.526           | 0.013               | 60.0            | 10.413            | 0.019              | V3      |
| rs121        | 094040+1205  | 145.1700               | 12.0970                | ...                     | ...                     | ...             | ...                | ...              | ...                 | 30.0            | 14.101            | 0.203              | MI      |
| rs122        | 094259+0929  | 145.7213               | 9.4923                 | 145.722443              | 9.494324                | 16.7            | 0.32               | 13.896           | 0.059               | 40.0            | 13.116            | 0.120              | V3      |
| rs123        | 094641+2407  | 146.6742               | 24.1240                | ...                     | ...                     | 7.0             | 1.0                | 15.423           | 0.171               | 50.0            | 13.729            | 0.255              | V2      |
| rs124        | 094744+2343  | 146.9544               | 23.7221                | 146.954193              | 23.722757               | 17.0            | 0.68               | 12.982           | 0.038               | 30.0            | 12.555            | 0.043              | V3      |
| rs125        | 095413+2806  | 148.5571               | 28.1000                | ...                     | ...                     | 1.8             | 1.0                | 18.200           | ...                 | ...             | ...               | ...                | NM      |
| rs126        | 100352+1105  | 150.9700               | 11.0980                | ...                     | ...                     | 4.1             | 0.8                | 16.700           | ...                 | ...             | ...               | ...                | NM      |
| rs127        | 100500+2132  | 151.2521               | 21.5380                | ...                     | ...                     | 10.4            | 0.34               | 15.427           | 0.117               | 40.0            | 14.728            | 0.363              | V2      |
| rs128        | 100508+2207  | 151.2871               | 22.1270                | 151.284830              | 22.119650               | 3.0             | 0.7                | 17.800           | ...                 | 10.0            | 15.4              | ...                | MI      |
| rs129        | 100735+1306  | 151.8971               | 13.1100                | 151.888080              | 13.106690               | 6.0             | 1.0                | 16.000           | ...                 | 20.0            | 14.9              | ...                | MI      |
| rs130        | 101421+2207  | 153.5906               | 22.1249                | 153.590363              | 22.124683               | 21.7            | 0.26               | 13.295           | 0.037               | 40.0            | 12.421            | 0.053              | V3      |
| rs131        | 101636+2107  | 154.1424               | 21.1229                | 154.142334              | 21.122868               | 29.3            | 0.80               | 10.293           | 0.009               | 40.0            | 10.217            | 0.007              | V3      |
| rs132        | 101903+2209  | 154.7650               | 22.1520                | 154.765000              | 22.152000               | ...             | ...                | ...              | ...                 | ...             | ...               | ...                | NM      |
| rs133        | 102055+2009  | 155.2329               | 20.1540                | 155.233246              | 20.155014               | 7.0             | 0.26               | 16.929           | 0.297               | 60.0            | 14.033            | 0.346              | V2      |
| rs134        | 102517+2007  | 156.3242               | 20.1240                | ...                     | ...                     | 4.0             | 1.0                | 17.4             | ...                 | ...             | ...               | ...                | NM      |
| rs135        | 102714+2531  | 156.8159               | 25.5187                | 156.815552              | 25.518274               | 7.0             | 1.00               | 15.377           | 0.113               | 25.0            | 14.424            | 0.182              | V3      |
| rs136        | 102830+1933  | 157.1250               | 19.5610                | 157.125830              | 19.561620               | 3.5             | 1.0                | 17.0             | ...                 | 15.0            | 15.7              | ...                | MI      |
| rs137        | 102922+2605  | 157.3198               | 26.0993                | 157.320038              | 26.099096               | 49.5            | 0.26               | 10.891           | 0.013               | 30.0            | 10.993            | 0.010              | V3      |
| rs138        | 103143+2518  | 157.9292               | 25.3100                | 157.930374              | 25.308094               | 7.0             | 0.24               | 17.199           | 0.290               | 60.0            | 13.519            | 0.169              | V2      |
| rs139        | 103439+2305  | 158.6658               | 23.0900                | 158.666000              | 23.090010               | 1.1             | 1.0                | 19.3             | ...                 | 40.0            | 14.0              | ...                | MI      |
| rs140        | 103542+2607  | 158.9250               | 26.1260                | 158.925232              | 26.126038               | 14.5            | 0.58               | 13.244           | 0.037               | 30.0            | 12.955            | 0.062              | V3      |
| rs141        | 103937+2519  | 159.9127               | 25.3225                | 159.912598              | 25.322615               | 15.6            | 0.82               | 12.380           | 0.034               | 40.0            | 12.008            | 0.053              | V3      |
| rs142        | 104208+2344  | 160.5459               | 23.7464                | 160.546112              | 23.746815               | 17.0            | 0.94               | 11.836           | 0.018               | 30.0            | 11.674            | 0.019              | V3      |
| rs143        | 104310+1330  | 160.7950               | 13.5130                | 160.773958              | 13.510869               | ...             | ...                | ...              | ...                 | 30.0            | 14.8              | ...                | MI      |
| rs144        | 104702+2632  | 161.7614               | 26.5432                | 161.760864              | 26.542980               | 18.5            | 0.82               | 12.412           | 0.032               | 30.0            | 12.150            | 0.032              | V3      |
| rs145        | 104722+1404  | 161.8429               | 14.0700                | 161.845993              | 14.068090               | 7.0             | 1.0                | 15.822           | 0.164               | 70.0            | 12.153            | 0.053              | V2      |
| rs146        | 104829+1232  | 162.1221               | 12.5350                | 162.116226              | 12.533339               | 62.1            | 0.4                | 10.506           | 0.007               | 70.0            | 10.288            | 0.010              | V2      |
| rs147        | 104916+1226  | 162.3171               | 12.4350                | 162.322479              | 12.420360               | 12.0            | 0.36               | 15.359           | 0.109               | 50.0            | 13.963            | 0.209              | V2      |
| rs148        | 104954+1309  | 162.4677               | 13.1619                | 162.467484              | 13.161813               | 7.0             | 1.00               | 14.915           | 0.072               | 25.0            | 14.681            | 0.220              | V3      |
| rs149        | 105204+1008  | 163.0165               | 10.1482                | 163.015945              | 10.148239               | 33.8            | 0.78               | 11.041           | 0.032               | 70.0            | 10.288            | 0.030              | V3      |
| rs150        | 110331+1107  | 165.8829               | 11.1210                | 165.885040              | 11.120287               | 8.0             | 0.24               | 16.637           | 0.353               | 60.0            | 13.211            | 0.213              | V2      |

Table 1—Continued

| ADBS<br>Num. | ADBS<br>Name | $\alpha_{ADBS}$<br>deg | $\delta_{ADBS}$<br>deg | $\alpha_{2MASS}$<br>deg | $\delta_{2MASS}$<br>deg | $R_{J21e}$<br>" | b/a $_{J21}$ | $J_{21e}$ | err $_{J21e}$ | $R_{Aper}$<br>"    | $J_{Aper}$ | err $_{J_{Ap}}$ | Method. |
|--------------|--------------|------------------------|------------------------|-------------------------|-------------------------|-----------------|--------------|-----------|---------------|--------------------|------------|-----------------|---------|
| rs151        | 110710+1834  | 166.7950               | 18.5720                | 166.791351              | 18.569765               | ...             | ...          | ...       | ...           | 50.0               | 13.451     | 0.161           | V2      |
| rs152        | 110742+1933  | 166.9250               | 19.5510                | 166.943451              | 19.549334               | ...             | ...          | ...       | ...           | 70.0               | 12.726     | 0.113           | V2      |
| rs153        | 111027+1007  | 167.6150               | 10.1260                | 167.605780              | 10.126110               | 5.0             | 1.0          | 16.3      | ...           | 15.0               | 15.0       | ...             | MI      |
| rs154        | 111032+1932  | 167.6342               | 19.5390                | 167.656250              | 19.538505               | ...             | ...          | ...       | ...           | ...                | ...        | ...             | NM      |
| rs155        | 111341+2131  | 168.4577               | 21.5213                | 168.457855              | 21.520327               | 10.7            | 0.52         | 14.643    | 0.088         | 25.0               | 13.454     | 0.095           | V3      |
| rs156        | 111852+1305  | 169.7330               | 13.0942                | 169.730515              | 13.092888               | 80.0            | 0.68         | 7.509     | 0.001         | 286.1 <sup>1</sup> | 6.989      | 0.016           | V2      |
| rs157        | 112020+1259  | 170.0630               | 12.9932                | 170.062531              | 12.989819               | 80.0            | 0.74         | 7.516     | 0.002         | 279.6 <sup>1</sup> | 6.835      | 0.016           | V2      |
| rs158        | 112026+1334  | 170.0706               | 13.5876                | 170.067947              | 13.590096               | 61.6            | 0.38         | 10.108    | 0.018         | 478.7 <sup>1</sup> | 7.174      | 0.020           | V2      |
| rs159        | 112134+2010  | 170.4303               | 20.1691                | 170.429611              | 20.169542               | 79.1            | 0.64         | 9.544     | 0.018         | 105.0 <sup>1</sup> | 9.431      | 0.016           | V3      |
| rs160        | 112914+2035  | 172.3138               | 20.5833                | 172.313721              | 20.583197               | 18.3            | 0.38         | 13.601    | 0.065         | 40.0               | 12.905     | 0.114           | V3      |
| rs161        | 112949+2207  | 172.4384               | 22.1268                | 172.438293              | 22.126610               | 18.8            | 0.76         | 12.588    | 0.041         | 40.0               | 12.280     | 0.060           | V3      |
| rs162        | 113115+2530  | 172.8418               | 25.5009                | 172.841888              | 25.501511               | 12.4            | 0.34         | 14.883    | 0.098         | 20.0               | 14.226     | 0.153           | V3      |
| rs163        | 113119+2306  | 172.8292               | 23.1160                | 172.838943              | 23.114342               | 7.8             | 0.18         | 16.774    | 0.237         | 50.0               | 14.331     | 0.378           | V2      |
| rs164        | 113816+1206  | 174.5540               | 12.1123                | 174.553879              | 12.112137               | 24.6            | 0.92         | 11.766    | 0.017         | 60.0               | 11.509     | 0.035           | V2      |
| rs165        | 113845+2008  | 174.6887               | 20.1430                | ...                     | ...                     | 10.2            | 0.4          | 14.2      | ...           | ...                | ...        | ...             | NM      |
| rs166        | 114101+1128  | 175.2441               | 11.4707                | 175.244736              | 11.471132               | 66.9            | 0.74         | 9.043     | 0.014         | 109.4 <sup>1</sup> | 8.843      | 0.016           | V3      |
| rs167        | 114227+2007  | 175.6021               | 20.1192                | 175.602005              | 20.119471               | 17.4            | 0.66         | 12.123    | 0.024         | 30.0               | 11.918     | 0.029           | V3      |
| rs168        | 114921+2607  | 177.3279               | 26.1215                | 177.328110              | 26.121529               | 29.7            | 0.60         | 11.696    | 0.031         | 50.0               | 11.424     | 0.039           | V3      |
| rs169        | 115004+2628  | 177.5191               | 26.4800                | 177.518539              | 26.478996               | 36.4            | 0.48         | 11.035    | 0.015         | 60.0               | 10.837     | 0.022           | V3      |
| rs170        | 115040+2531  | 177.6679               | 25.5260                | 177.666140              | 25.526370               | 6.1             | 0.6          | 15.9      | ...           | 15.0               | 15.1       | ...             | MI      |
| rs171        | 115840+2519  | 179.6695               | 25.3158                | 179.669601              | 25.316420               | 34.8            | 0.22         | 11.879    | 0.020         | 30.0               | 11.809     | 0.023           | V3      |
| rs172        | 115843+2506  | 179.6817               | 25.1164                | ...                     | ...                     | 1.5             | 1.0          | 18.8      | ...           | ...                | ...        | ...             | NM      |
| rs173        | 115906+2428  | 179.7771               | 24.4690                | 179.774933              | 24.472343               | 7.0             | 1.0          | 16.276    | 0.285         | 40.0               | 14.739     | 0.394           | V2      |
| rs174        | 120033+2004  | 180.1362               | 20.0741                | 180.136734              | 20.073902               | 28.8            | 0.86         | 11.340    | 0.037         | 60.0               | 11.026     | 0.042           | V3      |
| rs175        | 120112+1406  | 180.2932               | 14.1045                | 180.293259              | 14.104513               | 27.8            | 0.28         | 12.552    | 0.030         | 40.0               | 12.279     | 0.051           | V3      |
| rs176        | 120351+2525  | 180.9740               | 25.4334                | 180.973862              | 25.434111               | 12.4            | 0.50         | 14.261    | 0.064         | 30.0               | 13.082     | 0.072           | V3      |
| rs177        | 121206+2518  | 183.0279               | 25.3120                | 183.027756              | 25.309816               | 7.0             | 1.0          | 16.379    | 0.330         | 25.0               | 15.390     | 0.474           | V2      |
| rs178        | 121233+1207  | 183.1347               | 12.1237                | 183.134674              | 12.123732               | 36.3            | 0.64         | 11.571    | 0.034         | 70.0               | 10.978     | 0.041           | V3      |
| rs179        | 121437+1205  | 183.6542               | 12.1000                | 183.637333              | 12.103053               | ...             | ...          | ...       | ...           | ...                | ...        | ...             | NM      |
| rs180        | 121514+1259  | 183.8199               | 13.0236                | 183.82016               | 13.023854               | 81.8            | 0.18         | 10.662    | 0.009         | 170.3 <sup>1</sup> | 10.320     | 0.028           | V2      |
| rs181        | 121516+2038  | 183.8093               | 20.6593                | 183.809830              | 20.659077               | 35.7            | 0.28         | 12.605    | 0.050         | 60.0               | 11.593     | 0.057           | V3      |
| rs182        | 121555+1308  | 183.9745               | 13.1490                | 183.975906              | 13.149279               | 90.8            | 0.4          | 8.350     | 0.001         | 317.8 <sup>1</sup> | 7.525      | 0.016           | V2      |
| rs183        | 122126+1130  | 185.3244               | 11.5107                | 185.324112              | 11.511108               | 50.5            | 0.40         | 10.947    | 0.033         | 101.2 <sup>1</sup> | 10.580     | 0.044           | V3      |
| rs184        | 122140+1130  | 185.4199               | 11.5028                | 185.419010              | 11.502320               | 31.1            | 1.0          | 11.4      | ...           | 60.0               | 11.1       | ...             | V3      |
| rs185        | 122647+1133  | 186.6958               | 11.5550                | 186.714035              | 11.554358               | 7.0             | 1.0          | 15.681    | 0.291         | 30.0               | 15.237     | 0.828           | V2      |
| rs186        | 123119+1129  | 187.8456               | 11.4927                | 187.846405              | 11.492820               | 13.0            | 0.44         | 14.074    | 0.094         | 30.0               | 13.713     | 0.224           | V3      |
| rs187        | 123352+1510  | 188.4700               | 15.1760                | 188.453491              | 15.168147               | 7.9             | 0.8          | 13.602    | 0.026         | 70.0               | 11.543     | 0.038           | V2      |
| rs188        | 123546+2801  | 188.9891               | 27.9615                | 188.991333              | 27.959259               | 80.0            | 0.6          | 8.832     | 0.004         | 315.0 <sup>1</sup> | 8.411      | 0.033           | V2      |
| rs189        | 123606+2602  | 189.0868               | 25.9873                | 189.086685              | 25.987391               | ...             | ...          | ...       | ...           | 325.6 <sup>1</sup> | 7.161      | 0.016           | V3      |
| rs190        | 124020+1031  | 190.0694               | 10.5185                | 190.069168              | 10.518446               | 13.8            | 0.94         | 12.935    | 0.061         | 40.0               | 12.630     | 0.116           | V3      |
| rs191        | 124358+1307  | 190.9873               | 13.1268                | 190.98616               | 13.126577               | 93.0            | 0.58         | 8.949     | 0.005         | 190.5 <sup>1</sup> | 8.647      | 0.020           | V2      |
| rs192        | 124412+1207  | 191.0521               | 12.1170                | ...                     | ...                     | 2.8             | 1.0          | 17.1      | ...           | ...                | ...        | ...             | NM      |
| rs193        | 124516+2708  | 191.3209               | 27.1252                | 191.321457              | 27.125490               | 26.9            | 0.70         | 11.409    | 0.021         | 50.0               | 11.139     | 0.027           | V3      |
| rs194        | 124820+0829  | 192.0962               | 8.4877                 | 192.095566              | 8.487244                | 94.6            | 0.56         | 8.540     | 0.013         | 117.7 <sup>1</sup> | 8.403      | 0.012           | V3      |
| rs195        | 124930+2528  | 192.3922               | 25.4696                | 192.392548              | 25.469921               | 37.9            | 0.44         | 11.475    | 0.028         | 70.0               | 11.022     | 0.044           | V3      |
| rs196        | 125029+2530  | 192.6100               | 25.5004                | 192.610886              | 25.500759               | 80.0            | 0.84         | 7.928     | 0.002         | 364.5 <sup>1</sup> | 7.160      | 0.024           | V2      |
| rs197        | 125145+2607  | 192.9408               | 26.1180                | 192.935074              | 26.109131               | 7.0             | 1.0          | 16.422    | 0.444         | 50.0               | 13.696     | 0.257           | V2      |
| rs198        | 125156+1205  | 192.9799               | 12.0837                | 192.980713              | 12.083027               | 53.6            | 0.24         | 10.632    | 0.021         | 70.0               | 10.547     | 0.040           | V3      |
| rs199        | 125223+2138  | 193.0992               | 21.6370                | ...                     | ...                     | 1.8             | 1.0          | 18.3      | ...           | ...                | ...        | ...             | NM      |
| rs200        | 125411+2709  | 193.5199               | 27.1476                | 193.521866              | 27.149630               | 7.0             | 1.0          | 15.903    | 0.254         | 60.0               | 13.158     | 0.173           | V2      |



Table 1—Continued

| ADBS<br>Num. | ADBS<br>Name | $\alpha_{ADBS}$<br>deg | $\delta_{ADBS}$<br>deg | $\alpha_{2MASS}$<br>deg | $\delta_{2MASS}$<br>deg | $R_{J21e}$<br>" | b/a <sub>J21</sub> | J <sub>21e</sub> | err <sub>J21e</sub> | $R_{Aper}$<br>"    | J <sub>Aper</sub> | err <sub>JAp</sub> | Method. |
|--------------|--------------|------------------------|------------------------|-------------------------|-------------------------|-----------------|--------------------|------------------|---------------------|--------------------|-------------------|--------------------|---------|
| rs251        | 184335+2011  | 280.8967               | 20.1913                | ...                     | ...                     | 5.0             | 1.0                | 16.3             | ...                 | ...                | ...               | ...                | NM      |
| rs252        | 184829+1835  | 282.1221               | 18.5960                | 282.122480              | 18.597260               | ...             | ...                | ...              | ...                 | ...                | ...               | ...                | NM      |
| rs253        | 192728+2012  | 291.8679               | 20.2060                | 291.867917              | 20.206000               | ...             | ...                | ...              | ...                 | ...                | ...               | ...                | NM      |
| rs254        | 202344+0832  | 305.9371               | 8.5390                 | 305.960780              | 8.538410                | 3.5             | 1.0                | 16.3             | ...                 | 25.0               | 14.3              | ...                | MI      |
| rs255        | 210538+2709  | 316.4092               | 27.1520                | 316.406042              | 27.152461               | ...             | ...                | ...              | ...                 | 7.0                | 16.4              | ...                | MI      |
| rs256        | 211113+2809  | 317.8050               | 28.1590                | ...                     | ...                     | 2.4             | 1.0                | 17.4             | ...                 | ...                | ...               | ...                | NM      |
| rs257        | 214731+2209  | 326.8808               | 22.1650                | 326.879050              | 22.164010               | 3.6             | 0.6                | 17.1             | ...                 | 10.0               | 15.7              | ...                | MI      |
| rs258        | 214813+2209  | 327.0547               | 22.1591                | 327.054321              | 22.159580               | 32.2            | 0.88               | 10.660           | 0.018               | 60.0               | 10.437            | 0.020              | V3      |
| rs259        | 223744+2347  | 339.4458               | 23.7863                | 339.445374              | 23.786671               | 74.7            | 0.22               | 9.745            | 0.012               | 107.6 <sup>1</sup> | 9.693             | 0.012              | V3      |
| rs260        | 225557+2610  | 343.9879               | 26.1710                | ...                     | ...                     | 2.3             | 1.0                | 17.9             | ...                 | ...                | ...               | ...                | NM      |
| rs261        | 230433+2709  | 346.1400               | 27.1560                | 346.140320              | 27.155710               | 14.4            | 0.44               | 14.643           | 0.104               | 25.0               | 14.008            | 0.151              | V2      |
| rs262        | 231941+1011  | 349.9228               | 10.1852                | 349.922363              | 10.184981               | 17.1            | 0.66               | 12.794           | 0.052               | 60.0               | 11.481            | 0.067              | V3      |
| rs263        | 234042+2613  | 355.1758               | 26.2320                | 355.166138              | 26.236441               | 8.2             | 0.36               | 15.789           | 0.172               | 70.0               | 12.106            | 0.081              | V2      |
| rs264        | 234734+1836  | 356.8950               | 18.6000                | 356.922119              | 18.600136               | 8.2             | 0.34               | 16.266           | 0.240               | 30.0               | 13.898            | 0.166              | V2      |
| rs265        | 235121+2034  | 357.8278               | 20.5778                | 357.827637              | 20.577906               | 13.6            | 0.40               | 14.137           | 0.064               | 25.0               | 13.729            | 0.117              | V3      |

<sup>1</sup>Sources significantly larger than 70'' have J-band extrapolated magnitudes and sizes substituted for the aperture values because the 70'' aperture values are severe underestimates of the sizes and fluxes of the systems.

Table 2. 2MASS Data for AS Galaxies

| AS<br>Name | $\alpha_{AS}$<br>deg | $\delta_{AS}$<br>deg | $\alpha_{2MASS}$<br>deg | $\delta_{2MASS}$<br>deg | $R_{J21e}$<br>" | b/a $_{J21}$ | $J_{21e}$ | err $_{J21e}$ | $R_{Aper}$<br>" | $J_{Aper}$ | err $_{JAper}$ | Meas. |
|------------|----------------------|----------------------|-------------------------|-------------------------|-----------------|--------------|-----------|---------------|-----------------|------------|----------------|-------|
| SS01       | 331.1152             | 23.3133              | 331.1197                | 23.3204                 | ...             | ...          | ...       | ...           | 15.0            | 14.6       | ...            | MI    |
| SS02       | 337.0285             | 23.3737              | ...                     | ...                     | ...             | ...          | ...       | ...           | 7.0             | 17.7       | ...            | MI    |
| SS03       | 340.3504             | 23.3751              | 340.3521                | 23.3755                 | 13.6            | 0.76         | 13.19     | 0.053         | 25.0            | 12.873     | 0.066          | V3    |
| SS04       | 344.7468             | 24.0036              | 344.7480                | 24.0038                 | 15.3            | 0.26         | 14.28     | 0.079         | 25.0            | 13.837     | 0.159          | V3    |
| SS05       | 345.9213             | 23.6856              | ...                     | ...                     | 2.6             | 1.0          | 17.5      | ...           | 20.0            | 14.7       | ...            | MI    |
| SS06       | 347.0237             | 23.2605              | ...                     | ...                     | ...             | ...          | ...       | ...           | ...             | ...        | ...            | NM    |
| SS07       | 347.1364             | 23.6312              | ...                     | ...                     | 7.2             | 1.0          | 15.3      | ...           | 40.0            | 14.3       | ...            | MI    |
| SS08       | 350.2188             | 23.8071              | 350.2199                | 23.8074                 | 33.9            | 0.16         | 12.04     | 0.021         | 25.0            | 12.040     | 0.026          | V3    |
| SS09       | 350.6530             | 23.3747              | 350.6534                | 23.3747                 | 8.8             | 0.86         | 14.40     | 0.075         | 25.0            | 13.817     | 0.128          | V3    |
| SS10       | 351.0689             | 23.8434              | ...                     | ...                     | ...             | ...          | ...       | ...           | ...             | ...        | ...            | NM    |
| SS11       | 351.1405             | 23.9862              | 351.1415                | 23.9866                 | 15.5            | 0.24         | 14.45     | 0.091         | 25.0            | 13.819     | 0.166          | V3    |
| SS12       | 351.9209             | 23.5888              | 351.9210                | 23.5889                 | 24.7            | 0.62         | 11.66     | 0.027         | 40.0            | 11.411     | 0.031          | V3    |
| SS13       | 352.0248             | 23.5313              | 352.0260                | 23.5314                 | 17.6            | 0.96         | 11.43     | 0.021         | 30.0            | 11.311     | 0.021          | V3    |
| SS14       | 352.9108             | 24.0364              | ...                     | ...                     | ...             | ...          | ...       | ...           | ...             | ...        | ...            | NM    |
| SS15       | 353.0082             | 23.5579              | 353.0090                | 23.5574                 | 13.2            | 0.72         | 13.00     | 0.041         | 30.0            | 12.782     | 0.071          | V3    |
| SS16       | 353.1212             | 23.9311              | 353.1211                | 23.9310                 | 28.5            | 0.68         | 10.80     | 0.016         | 50.0            | 10.690     | 0.021          | V3    |
| SS17       | 353.6124             | 23.9037              | 353.6132                | 23.9032                 | 7.0             | 1.0          | 15.36     | 0.145         | 15.0            | 14.845     | 0.192          | V2    |
| SS18       | 353.6850             | 23.9713              | ...                     | ...                     | ...             | ...          | ...       | ...           | ...             | ...        | ...            | NM    |
| SS19       | 353.9638             | 23.6187              | 353.9651                | 23.6187                 | 22.4            | 0.80         | 11.56     | 0.026         | 40.0            | 11.431     | 0.031          | V3    |
| SS20       | 355.8094             | 23.5113              | 355.8094                | 23.5118                 | 15.9            | 0.30         | 13.85     | 0.054         | 25.0            | 13.692     | 0.109          | V3    |
| SS21       | 355.8252             | 23.5131              | 355.8263                | 23.5114                 | ...             | ...          | ...       | ...           | ...             | ...        | ...            | NM    |
| SS22       | 0.4081               | 23.4845              | 0.4096                  | 23.4836                 | 41.9            | 0.38         | 10.62     | 0.017         | 70.0            | 10.100     | 0.022          | V3    |
| SS23       | 0.4232               | 23.4970              | 0.4247                  | 23.4958                 | 30.2            | 0.38         | 11.26     | 0.020         | 40.0            | 11.118     | 0.024          | V3    |
| SS24       | 1.2792               | 23.9720              | 1.2701                  | 23.9694                 | 7.0             | 0.6          | 15.3      | ...           | 20.0            | 14.7       | ...            | MI    |
| SS25       | 1.5939               | 23.7889              | 1.5952                  | 23.7894                 | 14.2            | 0.36         | 14.35     | 0.085         | 25.0            | 13.661     | 0.125          | V3    |
| SS26       | 2.2257               | 23.8174              | 2.2279                  | 23.8169                 | 19.4            | 0.50         | 12.97     | 0.050         | 25.0            | 12.729     | 0.055          | V3    |
| SS27       | 3.4943               | 23.9691              | 3.4941                  | 23.9700                 | 11.8            | 0.50         | 14.19     | 0.075         | 30.0            | 13.366     | 0.122          | V3    |
| SS28       | 4.7505               | 23.4782              | 4.7523                  | 23.4765                 | 12.2            | 0.64         | 13.66     | 0.056         | 30.0            | 13.115     | 0.092          | V3    |
| SS29       | 5.5197               | 23.7365              | 5.5212                  | 23.7369                 | 16.6            | 0.52         | 13.36     | 0.058         | 30.0            | 12.893     | 0.079          | V3    |
| SS30       | 6.4859               | 23.9238              | ...                     | ...                     | ...             | ...          | ...       | ...           | ...             | ...        | ...            | NM    |
| SS31       | 6.8649               | 23.7228              | 6.8655                  | 23.7234                 | 10.4            | 0.34         | 15.312    | 0.149         | 15.0            | 14.919     | 0.256          | V2    |
| SS32       | 8.1336               | 23.3954              | 8.1351                  | 23.3951                 | 14.1            | 0.42         | 14.04     | 0.077         | 30.0            | 13.181     | 0.108          | V3    |
| SS33       | 8.3984               | 23.3981              | 8.3996                  | 23.3977                 | 17.5            | 0.48         | 13.27     | 0.058         | 40.0            | 12.815     | 0.113          | V3    |
| SS34       | 8.9901               | 24.0374              | 8.9913                  | 24.0370                 | 13.5            | 0.36         | 14.35     | 0.083         | 25.0            | 13.740     | 0.141          | V3    |
| SS35       | 9.0151               | 23.9582              | 9.0168                  | 23.9578                 | 31.6            | 0.84         | 10.71     | 0.019         | 70.0            | 10.322     | 0.025          | V3    |
| SS36       | 9.2147               | 23.9914              | 9.2150                  | 23.9909                 | 32.6            | 0.76         | 10.39     | 0.015         | 60.0            | 10.196     | 0.018          | V3    |
| SS37       | 10.7042              | 23.4903              | 10.7041                 | 23.4901                 | 20.9            | 0.38         | 12.31     | 0.030         | 25.0            | 12.168     | 0.035          | V3    |
| SS38       | 10.7271              | 23.5031              | 10.7271                 | 23.5030                 | 20.8            | 0.66         | 11.83     | 0.027         | 40.0            | 11.503     | 0.034          | V3    |
| SS39       | 11.2149              | 23.8069              | ...                     | ...                     | ...             | ...          | ...       | ...           | ...             | ...        | ...            | NM    |
| SS40       | 12.4269              | 24.0459              | 12.4288                 | 24.0455                 | 9.2             | 0.74         | 13.47     | 0.043         | 20.0            | 13.154     | 0.065          | V3    |
| SS41       | 12.98                | 23.48                | ...                     | ...                     | 5.5             | 1.0          | 15.3      | ...           | 20.0            | 14.6       | ...            | MI    |
| SS42       | 14.0674              | 24.0538              | ...                     | ...                     | ...             | ...          | ...       | ...           | ...             | ...        | ...            | NM    |
| SS43       | 14.3303              | 23.8899              | 14.3321                 | 23.8899                 | 13.9            | 0.52         | 13.78     | 0.059         | 30.0            | 13.181     | 0.091          | V3    |
| SS44       | 19.9940              | 23.9652              | 19.9950                 | 23.9647                 | 7.0             | 1.0          | 15.216    | 0.130         | 20.0            | 14.449     | 0.182          | V2    |
| SS45       | 22.8405              | 23.9544              | ...                     | ...                     | ...             | ...          | ...       | ...           | 25.0            | 15.1       | ...            | MI    |
| SS46       | 23.7908              | 24.0077              | ...                     | ...                     | 6.6             | 1.0          | 15.2      | ...           | 15.0            | 14.9       | ...            | MI    |
| SS47       | 24.1481              | 23.8156              | ...                     | ...                     | ...             | ...          | ...       | ...           | ...             | ...        | ...            | NM    |
| SS48       | 26.2821              | 23.7699              | ...                     | ...                     | ...             | ...          | ...       | ...           | 15.0            | 15.8       | ...            | MI    |
| SS49       | 27.6763              | 23.4003              | 27.6777                 | 23.3993                 | 9.8             | 0.42         | 14.49     | 0.060         | 20.0            | 14.219     | 0.140          | V3    |
| SS50       | 28.4721              | 23.9116              | 28.4742                 | 23.9141                 | ...             | ...          | ...       | ...           | 15.0            | 14.7       | ...            | MI    |
| SS51       | 29.9746              | 23.6448              | 29.9769                 | 23.6444                 | 36.7            | 0.68         | 10.82     | 0.021         | 60.0            | 10.546     | 0.023          | V3    |
| SS52       | 30.1886              | 23.7543              | ...                     | ...                     | ...             | ...          | ...       | ...           | 10.0            | 15.9       | ...            | MI    |
| SS53       | 30.2624              | 23.4191              | 30.2634                 | 23.4177                 | 12.6            | 0.72         | 13.26     | 0.044         | 30.0            | 13.029     | 0.083          | V3    |
| SS54       | 30.8369              | 23.7580              | 30.8365                 | 23.7612                 | 3.9             | 1.0          | 16.8      | ...           | 50.0            | 13.6       | ...            | MI    |
| SS55       | 30.9358              | 24.0252              | 30.9296                 | 24.0286                 | 6.1             | 0.5          | 15.3      | ...           | 30.0            | 13.8       | ...            | MI    |
| SS56       | 32.2781              | 23.8435              | ...                     | ...                     | ...             | ...          | ...       | ...           | 20.0            | 15.5       | ...            | MI    |
| SS57       | 32.2964              | 23.2527              | 32.2977                 | 23.2521                 | 11.0            | 0.44         | 14.33     | 0.065         | 20.0            | 13.917     | 0.112          | V3    |
| SS58       | 33.4041              | 23.2470              | 33.4003                 | 23.2585                 | 2.5             | 0.6          | 17.1      | ...           | 10.0            | 15.8       | ...            | MI    |
| SS59       | 36.2982              | 23.8443              | 36.2925                 | 23.8517                 | 9.3             | 1.0          | 14.3      | ...           | 30.0            | 13.7       | ...            | MI    |
| SS60       | 36.3403              | 23.8285              | 36.3414                 | 23.8272                 | 11.7            | 0.80         | 13.33     | 0.047         | 30.0            | 13.026     | 0.084          | V3    |
| SS61       | 37.0907              | 23.2155              | 37.0923                 | 23.2146                 | 29.1            | 0.28         | 12.23     | 0.029         | 30.0            | 12.089     | 0.035          | V3    |
| SS62       | 37.1645              | 23.7972              | 37.1663                 | 23.7964                 | 15.0            | 0.66         | 12.65     | 0.032         | 25.0            | 12.355     | 0.036          | V3    |
| SS63       | 37.3371              | 23.9717              | 37.3392                 | 23.9705                 | 9.0             | 0.62         | 14.53     | 0.076         | 25.0            | 13.560     | 0.107          | V3    |
| SS64       | 38.1064              | 23.3647              | 38.1076                 | 23.6525                 | 3.1             | 0.8          | 16.6      | ...           | 15.0            | 15.2       | ...            | MI    |
| SS65       | 38.2242              | 23.3283              | 38.2242                 | 23.3276                 | 15.9            | 0.36         | 13.86     | 0.068         | 30.0            | 13.495     | 0.139          | V3    |
| SS66       | 38.3713              | 23.4862              | 38.3712                 | 23.4850                 | 12.6            | 0.36         | 14.783    | 0.098         | 25.0            | 13.887     | 0.147          | V2    |



Table 2—Continued

| AS<br>Name | $\alpha_{AS}$<br>deg | $\delta_{AS}$<br>deg | $\alpha_{2MASS}$<br>deg | $\delta_{2MASS}$<br>deg | $R_{J21e}$<br>" | $b/a_{J21}$ | $J_{21e}$ | $err_{J21e}$ | $R_{Aper}$<br>" | $J_{Aper}$ | $err_{JAp}$ | Meas. |
|------------|----------------------|----------------------|-------------------------|-------------------------|-----------------|-------------|-----------|--------------|-----------------|------------|-------------|-------|
| SS67       | 38.6782              | 23.4142              | 38.6797                 | 23.4131                 | 38.6            | 0.74        | 10.43     | 0.017        | 60.0            | 10.251     | 0.017       | V3    |
| SS68       | 39.0389              | 23.9003              | 39.0404                 | 23.8991                 | 18.4            | 0.56        | 13.10     | 0.050        | 50.0            | 12.230     | 0.077       | V3    |
| SS69       | 39.3623              | 23.3013              | 39.3645                 | 23.3000                 | 15.6            | 0.62        | 12.86     | 0.042        | 40.0            | 12.468     | 0.079       | V3    |
| SS70       | 40.3270              | 23.2694              | ...                     | ...                     | ...             | ...         | ...       | ...          | ...             | ...        | ...         | NM    |
| SS71       | 41.7268              | 23.5962              | 41.7276                 | 23.5956                 | 20.2            | 0.58        | 12.00     | 0.023        | 30.0            | 11.858     | 0.026       | V3    |
| SS72       | 41.9639              | 23.4062              | 41.9655                 | 23.4040                 | 29.3            | 0.44        | 11.80     | 0.025        | 60.0            | 11.480     | 0.048       | V3    |
| SS73       | 42.1616              | 23.2747              | ...                     | ...                     | ...             | ...         | ...       | ...          | ...             | ...        | ...         | NM    |
| SS74       | 43.6756              | 23.3781              | ...                     | ...                     | ...             | ...         | ...       | ...          | 15.0            | 16.0       | ...         | MI    |
| SS75       | 44.3925              | 23.7871              | ...                     | ...                     | ...             | ...         | ...       | ...          | 20.0            | 15.9       | ...         | MI    |

FIG. 1.— The ADBS galaxies in order of baryonic mass from the most massive to the least massive. (JPEG file included with download)

FIG. 2.— The ADBS galaxies for which baryonic mass was not able to be determined. (JPEG file included with download)

FIG. 3.— The AS galaxies in order of baryonic mass from the most massive to the least massive. (JPEG file included with download)

FIG. 4.— The AS galaxies for which baryonic mass was not able to be determined. (JPEG file included with download)

This figure "Rosenberg.figA1\_comp.jpg" is available in "jpg" format from:

<http://arxiv.org/ps/astro-ph/0411499v1>

This figure "Rosenberg.figA2\_comp.jpg" is available in "jpg" format from:

<http://arxiv.org/ps/astro-ph/0411499v1>

This figure "Rosenberg.figA3\_comp.jpg" is available in "jpg" format from:

<http://arxiv.org/ps/astro-ph/0411499v1>

This figure "Rosenberg.figA4\_comp.jpg" is available in "jpg" format from:

<http://arxiv.org/ps/astro-ph/0411499v1>

This figure "Rosenberg.figA5\_comp.jpg" is available in "jpg" format from:

<http://arxiv.org/ps/astro-ph/0411499v1>

This figure "Rosenberg.figA6\_comp.jpg" is available in "jpg" format from:

<http://arxiv.org/ps/astro-ph/0411499v1>